Mathematical Biosciences and Engineering

http://www.aimspress.com/journal/MBE

MBE, 23(6): 1534–1571.
DOI: 10.3934/mbe.2026056
Received: 17 November 2025
Revised: 21 March 2026
Accepted: 08 April 2026
Published: 20 April 2026

Research article

A multi-strain sequential super-infection model for dengue fever with antibody dependent enhancement

Taurai Mademutsa [1,*], Mark Kimathi [2], Jeconia Okello Abonyo [3] and Tinashe Byron Gashirai [4]

[1] Department of Mathematics, Pan African University Institute for Basic Sciences, Technology & Innovation, Nairobi, Kenya

[2] Department of Mathematics and Statistics, Machakos University, Nairobi, Kenya

[3] Department of Mathematics, Jomo Kenyatta University of Agricultural & Technology, Kenya

[4] Institute for Modeling Collaboration and Innovation (IMCI), University of Idaho, Idaho, USA

* **Correspondence:** Email: mademutsa.taurai@gmail.com.

Abstract: Dengue fever is a vector-borne disease that is transmitted by the *aedes aegypti* mosquito. The disease is caused by four different viral serotypes which are DEN-1, DEN-2, DEN-3, and DEN-4. Of these serotypes, DEN-1 and DEN-2 are the most prevalent, and their co-circulation presents complex disease dynamics due to the antibody-dependent enhancement (ADE) phenomenon as well as the cross-immunity interaction of these viral serotypes. In this study, we formulate a novel multi-strain sequential super-infection model that captures the primary and secondary infection dynamics with temporary cross immunity, asymptomatic infections, and enhancement in disease transmissibility due to antibody-dependent enhancement (ADE) upon heterologous reinfection. Our analyses revealed that significant secondary infections cause a backward bifurcation phenomena due to changes in the biting rate b, which maintains disease endemicity when the basic reproduction number is below unity. The implications of this phenomena are that intervention measures would need to target a critical threshold of $\mathcal{R}_0$ associated with b_c, below which we are assured of disease elimination. Numerical analysis showed that the values of b_c are highly influenced by changes in the ADE. Thus effective control of dengue fever requires intensified and sustained control methods that drive transmission below critical thresholds. The findings of this study shed light on critical insights in the design and implementation of eradication measures in dengue fever endemic regions.

Keywords: Antibody-dependant enhancement (ADE); bifurcation; cross-immunity; serotype

1. Introduction

Dengue fever, also known as breakbone fever, is a parasite-host-vector infectious disease. The disease is known to be endemic in urban areas in several countries that lie in the tropical and subtropical regions [1]. Despite efforts to combat the disease, the incidence of the disease has been increasing in endemic regions, and the disease has now spread to other countries due to climate change, human migration, and adaptability of the *aedes aegypti* mosquito [2]. The disease is one of the most prevalent of all human infections throughout the world. An estimated 390,000,000 individuals are infected with dengue fever on an annual basis, with 20,000 deaths recorded annually [3]. Several factors influence disease transmission and these include rainfall patterns, humidity, and temperature. These factors affect the survival of the *aedes aegypti* mosquitoes, which are the vector responsible for spreading the disease [4]. The immunity of human beings is another factor that impacts disease dynamics in areas where the disease's prevalence and transmission is moderate or intense. Over years of exposure, adult human beings in endemic areas develop immunity to a specific serotype of dengue fever once infected [5]. While the development of immunity to a specific strain does not alleviate the risk of contracting a different strain of dengue fever, it offers partial temporal cross-immunity. This short-term partial cross-immunity is believed to give rise to complex temporal dynamics in the incidence of dengue fever [6]. In the transmission of dengue fever, the role of sub-clinical infections cannot be understated. Studies have indicated that an understanding of sub-clinical infections in dengue fever dynamics could greatly impact the control of the disease [7]. This silent transmission of the disease complicates vaccination efforts, as vaccination in dengue fever is dependent on the previous state of infection with a different serotype [8]. Numerous mathematical models have been developed to explore the dynamics of dengue fever. A minimalistic two-strain model with antibody-dependent enhancement (ADE) and temporary cross-immunity has been developed, and ADE was established as the primary driver of annual oscillations, bifurcation, and chaotic dynamics [9]. The study, however, did not incorporate explicit vector dynamics, asymptomatic individuals, and seropositive vaccination. Mathematical models with loss of immunity from an initial stage have been developed, and the formation of a cusp bifurcation describing the transition from a disease free state into an endemic equilibrium was established in [10]. The study did not explicitly include vector dynamics, thus it was not informative on vector dynamics and the required control strategies. Also, it has been noted that subsequent infection with one strain of the virus only confers immunity against that particular type of the serotype and can cause a severe form of the disease known as Dengue hemorrhagic fever (DHF) and dengue shock syndrome (DSS) when one is then infected with a different strain of the disease [11]. A study by [12] illustrated that during a secondary dengue fever infection, the period of viremia is shorter and thus an individual will not be viremic in the critical phase which signals the onset of severe dengue. This is hypothesized to be due to cross-reactive immunity developed during the initial infection and the existence of antibodies. It was illustrated that the onset of severe cases of the infection corresponded to the onset of the critical phase of the disease in which viremia levels were noted to have been significantly decreased. In the control of dengue fever, vaccination has resulted in complications, as it increase the risk of severe dengue when seronegative individuals are vaccinated [13]. This complication necessitates the need for screening efforts during the vaccination process. In querying this assertion, it is imperative to formulate mathematical models involving parameters capturing the dynamics of vaccination involving seropositive individuals to determine their influence on the spread of the disease.

1.1. Background of the study

Of late, trends in the importance of sub-clinical infections have been suspected to play a critical role in the transmission of dengue fever. A study by [14] noted the understudy of the burden of asymptomatic dengue infections. The study concluded that the majority of dengue fever infections are sub-clinical and are likely to play a critical role in the transmission of the disease. In their paper, [15] investigated the effect of active case findings on dengue fever control. The developed model consisted of two classes of susceptible individuals, (the high risk and low risk classes), an exposed class, the asymptomatic and infectious class, a hospitalized class, and the recovered class. The findings of the study suggested that health authorities should pay more attention to the active finding of asymptomatic cases. A study by [16] investigated an optimal control problem with asymptomatic cases. Different combinations of the proposed control methods were analyzed, and the best method was found to be the use of treatment bed-nets, which drastically reduced infected mosquitoes as compared with the other control strategies and thus leading to a decrease asymptomatic and symptomatic individuals. The model, however, did not consider the duration of the immunity, as the cross-immunity in dengue fever is considered temporary and short-lived.

In this study, we present a mathematical model that mimics the multi-strain spread of dengue fever within the mosquito (vector) population and the human (host) population. The role of the asymptomatic individuals in the spread of the disease cannot be overlooked, since it is known that the infectious but asymptomatic play an important role in the transmission dynamics of dengue fever. Apart from spreading the disease unaware, these infected asymptomatic individuals are reported to constitute the majority of the pool of infectious individuals. To curb the spread of dengue fever, it is imperative for us to understand the multi-strain dynamics of dengue fever, as that will give us an understanding into how we can tailor interventions to control the disease dynamics. To this end, we further subdivide the infectious host population into two subcategories, namely the asymptomatic infectious individuals and the symptomatic infectious individuals. In addition to these subcategories, we introduce vaccination of seropositive individuals in a bid to understand how secondary infection dynamics influence the spread of the disease.

1.2. Model formulation

The existing multi-strain models [17] have examined the circulation of two strains of dengue fever without mention of the vaccination of seropositive individuals. Most of the studies revealed in our work were deterministic models; we, however, note that not many of them have explored the consequences of a combination of asymptomatic infections, vaccination of seropositive individuals, ADE, and sequential super-infection on the dynamics of dengue fever. Taking the aforementioned shortfalls in earlier developed models into account, we develop a novel mathematical model to model the epidemiological interactions between the host population and the vector population in the dynamics of dengue fever. Our model takes two strains of the disease into account, DEN-1 and DEN-2. Considering the niche partitioning of viruses in multi-strain models, without loss of generality, our model presents the dominant strain DEN-2 as the primary infection and DEN-1 as the secondary infection.

The formulation of the dengue fever model is guided by the following.

(i) The human population is partitioned into 10 non-overlapping subpopulations, namely; $S_p(t)$, $S_s(t)$, $A_p(t)$, $A_s(t)$, $I_p(t)$, $I_s(t)$, $I_h(t)$, $R_p(t)$, $R_s(t)$, and $V(t)$, denoting individuals susceptible to primary infection, individuals susceptible to secondary infection, asymptomatic primary infectious individuals, asymptomatic secondary infectious individuals, symptomatic primary infectious individuals, symptomatic secondary infectious individuals, non-infectious individuals hospitalized due to secondary infection, recovered primary individuals, recovered secondary individuals, and individuals vaccinated after recovery from the primary infection.

(ii) The vector population is subdivided into two epidemiology states, namely- the susceptible vector population, $S_v(t)$ and the infectious vector population, $I_v(t)$.

(iii) The appearance of new mosquito infections is assumed to be given by the standard incidence rate,

$$\lambda_v = \frac{b[\beta_{vp}(I_p + \eta A_p) + \beta_{vs}(I_s + \eta A_s)]}{N_h},$$

where η is the modification parameter for asymptomatic cases signifying the potential for asymptomatic individuals to spread the disease at a higher rate than symptomatic individuals. In this study, β_{vp} is the per capita transmission rate of the primary infection from humans to the vector, β_{vs} is the per capita transmission rate of the secondary infections from humans to the vector, β_{hp} is the per capita transmission rate of the vector to humans, and β_{hs} is the per capita transmission of secondary infection from the vector to humans.

(iv) On the other hand, the incidence rates for the host population are given separately for primary and secondary infections as follows. For the primary infection, the new cases are generated via the infection of susceptible primary individuals by infected mosquitoes through the force of infection, given by

$$\lambda_p = \frac{b\beta_{hp}I_v}{N_h},$$

and that of the secondary infection is given by

$$\lambda_s = \frac{b\phi\beta_{hs}I_v}{N_h},$$

where ϕ is the modification parameter for the ADE and b is the mosquito biting rate.

(v) Human beings and mosquitoes naturally die at a rate μ and μ_v, respectively. Mosquitoes do not recover but the hosts recover at different rates for asymptomatic and symptomatic primary and secondary infections.

The movement of the host population and the vector population from one compartment to another is shown by the compartmental design described in 1.3. The developed model differs from existing models in the literature in that it is a multi-strain sequential super-infection model, treating the initial infection in an individual as a primary infection and the subsequent infection as a secondary infection. Table 1 describes the model variables as incorporated in the compartmental model and in the system of differential equations.

1.3. Compartmental diagram

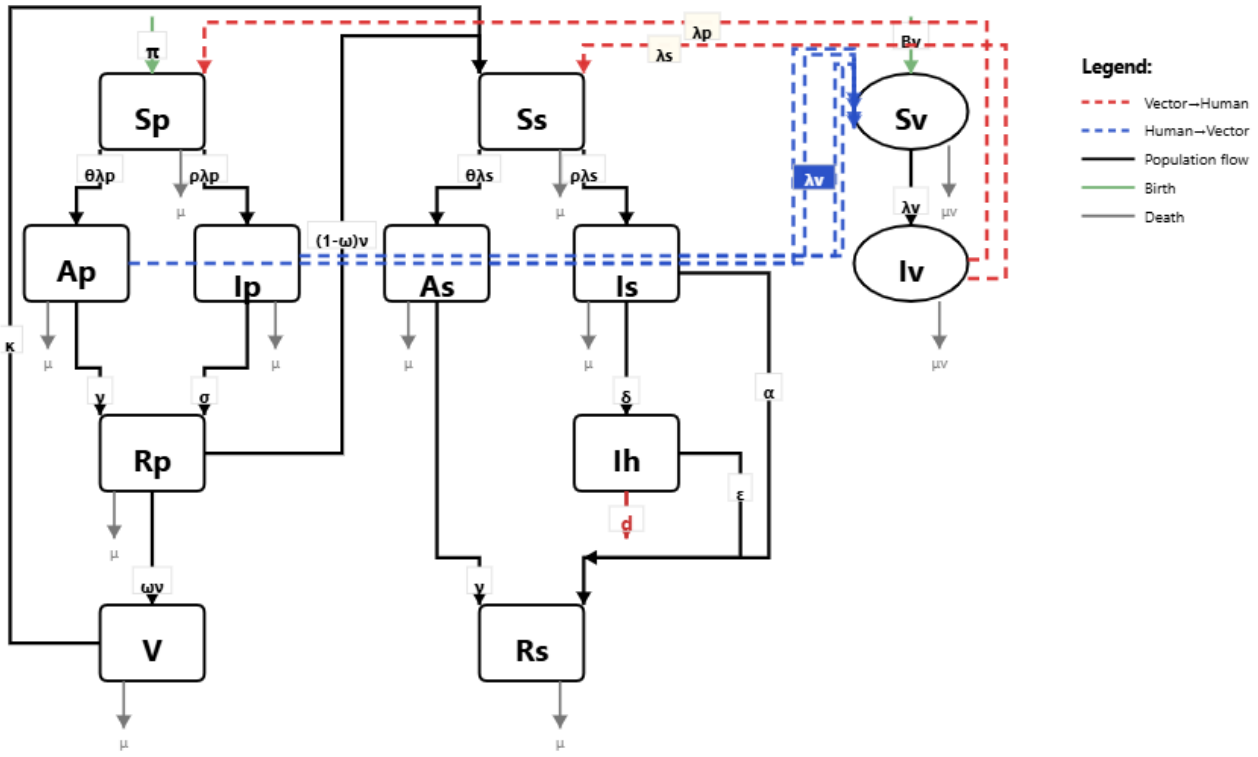

Figure 1. Compartmental flow diagram.

Table 1. Description of variables in the compartmental model.

Variable	Description
S_p	This is the class of people who are susceptible to a primary infection.
S_s	This is the class of people who are susceptible to a secondary infection.
A_p	This is the class of people who are asymptomatic with a primary infection.
A_s	This is the class of people who are asymptomatic with a secondary infection.
I_p	This is the class of people who are infectious with a primary infection.
I_s	This is the class of people who are infectious with a secondary infection.
R_p	This is the class of people who have recovered from a primary infection.
R_s	This is the class of people who have recovered from both infections.
V	This is the class of people who are vaccinated after recovery from a primary infection.
I_h	This is the class of people with severe dengue fever and are hospitalized.
S_v	This is the class of mosquitoes that are susceptible to the disease.
I_v	This is the class of mosquitoes that are infectious.

2. Model assumptions

The following assumptions govern our development of the dengue fever model.

1. The population is assumed to be homogeneous.
2. There is no vertical transmission of the infection in both the human and vector population.
3. Sub-clinical infections affect the dynamics of the disease.
4. There is increased susceptibility to a secondary infection due to ADE.
5. The human hosts' epidemiology acts on a much slower time scale than the vector due to their vastly different life-cycles.
6. There is co-infection in the vector population with biased virus transmission, which results in sequential-super-infection in the host population.

Therefore, the model that captures the dynamics of dengue fever incorporating the vaccination of seropositive individuals is given by the following system of ordinary differential equations:

$$\begin{cases} \frac{dS_p}{dt} = \pi - (\lambda_p + \mu)S_p \\ \frac{dA_p}{dt} = \theta\lambda_p S_p - (\mu + \gamma)A_p \\ \frac{dI_p}{dt} = \rho\lambda_p S_p - (\mu + \sigma)I_p \\ \frac{dR_p}{dt} = \gamma A_p + \sigma I_p - (\mu + \nu)R_p \\ \frac{dS_s}{dt} = (1-\omega)\nu R_p + \kappa V - (\lambda_s + \mu)S_s \\ \frac{dA_s}{dt} = \theta\lambda_s S_s - (\mu + \gamma)A_s \\ \frac{dI_s}{dt} = \rho\lambda_s S_s - (\mu + \alpha + \delta)I_s \\ \frac{dI_h}{dt} = \delta I_s - (\mu + \epsilon + d)I_h \\ \frac{dR_s}{dt} = \gamma A_s + \alpha I_s + \epsilon I_h - \mu R_s \\ \frac{dV}{dt} = \omega\nu R_p - (\mu + \kappa)V \\ \frac{dS_v}{dt} = B_v - (\lambda_v + \mu_v)S_v \\ \frac{dI_v}{dt} = \lambda_v S_v - \mu_v I_v \end{cases} \tag{2.1}$$

with the initial conditions given as

$S_p(0) \geq 0$, $A_p(0) \geq 0$, $I_p(0) \geq 0$, $R_p(0) \geq 0$, $S_S(0) \geq 0$, $A_s(0) \geq 0$, $I_s(0) \geq 0$, $I_h(0) \geq 0$, $R_s(0) \geq 0$, $V(0) \geq 0$, $S_v(0) \geq 0$, and $I_v(0) \geq 0$,

where the forces of infection λ_p, λ_s, and λ_v are given as

$$\lambda_p = \frac{b\beta_{hp}I_v}{N_h}, \qquad \lambda_s = \frac{b\phi\beta_{hs}I_v}{N_h}, \qquad \text{and} \qquad \lambda_v = \frac{b[\beta_{vp}(I_p+\eta A_p)+\beta_{vs}(I_s+\eta A_s)]}{N_h}.$$

Table 2. Description of parameters in the formulated model.

Parameter	Description
π	Constant recruitment rate for the human population.
μ	Natural death rate in the human population.
γ	Recovery rate for asymptomatic cases.
σ	Recovery rate for symptomatic cases.
α	Recovery rate for secondary infection.
ϵ	Rate of recovery from DHF.
η	Modification parameter for asymptomatic cases.
ω	Proportion of individuals who are vaccinated after recovery from a primary infection.
ν	Rate at which unvaccinated recovered individuals lose cross-immunity.
ϕ	ADE modification parameter.
θ	Proportion of infections that become asymptomatic.
ρ	Proportion of infections that become symptomatic.
b	Mosquito biting rate.
d	Proportion of people who die from DHF.
B_v	Constant recruitment rate for the mosquito population.
κ	Rate at which vaccinated individuals lose immunity after vaccine waning.
δ	Rate of hospitalization due to severe dengue.
μ_v	Natural death rate for the mosquito population.
β_{hp}	Per capita transmission rate of primary infection from the vector to humans.
β_{vp}	Per capita transmission rate of primary infection from humans to the vector.
β_{hs}	Per capita transmission rate of secondary infection from the vector to humans.
β_{vs}	Per capita transmission rate of secondary infection from humans to the vector.

3. Basic properties of the model

3.1. The invariant region

To determine if the proposed model is biologically feasible, the model variables are analyzed for positivity and boundedness. Thus, we postulate the following theorem.

Theorem 3.1. *The region $\mathbb{R}^{12}_+$ denoted by the closed set $D = D_h \cup D_v \in \mathbb{R}^{12}_+$ is positively invariant with respect to the above mentioned system of ordinary differential equations, and a non-negative solution exists for all $t > 0$ where*

$$D_h = \{(S_p(t), A_p(t), I_p(t), R_p(t), S_S(t), A_s(t), I_s(t), I_h(t), R_s(t)) \in \mathbb{R}^{10}_+ : N_h \leq \tfrac{\pi}{\mu}\} \text{ and}$$
$$D_v = \{(S_v(t), I_v(t) \in \mathbb{R}^2_+ : N_v \leq \tfrac{B_v}{\mu_v}\}.$$

Proof. The total change in the human population is given by

$$\frac{dN_h}{dt} = \frac{dS_p}{dt} + \frac{A_p}{dt} + \frac{dI_p}{dt} + \frac{dR_p}{dt} + \frac{dS_s}{dt} + \frac{dA_s}{dt} + \frac{I_s}{dt} + \frac{dI_h}{dt} + \frac{dR_s}{dt} + \frac{dV}{dt}.$$

Substituting for the model equations and simplifying yields

$$\frac{dN_h}{dt} = \pi - \mu N_h - dI_h \leq \pi - \mu N_h.$$

Solving the differential equation above by separating the variables yields

$$\int \frac{dN_h}{\pi - \mu N_h} \leq \int dt,$$

which simplifies to

$$\ln \left|\pi - \mu N_h\right| \leq -\mu t + c.$$

Solving for the initial conditions $t = 0$, $N_h = N_0$ implies that $A = \pi - \mu N_h$, which further implies that

$$\pi - \mu N_h \leq \left[\pi - \mu N_0\right] e^{-\mu t},$$

$$N_h \leq \frac{\pi}{\mu} + \left[N_0 - \frac{\pi}{\mu}\right] e^{-\mu t}.$$

As t approaches ∞, we have $0 \leq N_h \leq \frac{\pi}{\mu}$. □

Similarly, for the vector population, we deduce that the bounds on the total change in the population are given by $0 \leq N_v \leq \frac{B_v}{\mu_v}$ as t approaches ∞.

3.2. Positivity of solutions

A fundamental need for a biological model is that the solutions of the model must both be non-negative and bounded. It is therefore essential to show that the model variables remain positive whenever the time- t is greater than zero. Following this assertion, we arrive at the following theorem.

Theorem 3.2. *The solutions $S_p(t)$, $A_p(t)$, $I_p(t)$, $R_p(t)$, $S_S(t)$, $A_s(t)$, $I_s(t)$, $I_h(t)$, $R_s(t)$, $V(t)$, $S_v(t)$, and $I_v(t)$ of the given model with non-negative initial conditions remain non-negative for all $t > 0$ in D.*

Proof. Consider the first equation in Model 2.1. We have

$$\begin{aligned}
\tfrac{dS_p}{dt} &= \pi - \lambda_1 S_p - \mu S_p \\
\tfrac{dS_p}{dt} &= \pi - \lambda_1 S_p - \mu S_p \geq -(\lambda_1 + \mu) S_p \\
\tfrac{dS_p}{dt} &\geq -(\lambda_1 + \mu) S_p.
\end{aligned}$$

Separating variables and integrating yields $S_p \geq S_p(0) e^{-(\lambda_1+\mu)t} \geq 0$.

Therefore, the positivity of $S_p(t)$ is guaranteed. Similarly, for the remaining model variables in Model 2.1, we can conclude that the solution set of the given system is guaranteed to be non-negative for all $t > 0$ in the domain of feasibility D. □

4. Model equilibria

4.1. Disease-free equilibrium

The disease-free equilibrium point is defined as the point at which there is no disease in the population under study.

Thus, at the disease-free equilibrium point, the following condition holds at the steady state:

$A_p^*(t) = I_p^*(t) = R_p^*(t) = S_s^*(t) = A_s^*(t) = I_s^*(t) = I_h^*(t) = R_s^*(t) = V^*(t) = I_v^*(t) = 0$. while

$S_p^*(t) > 0, S_v^*(t) > 0$.

Consequently, setting Model 2.1 to zero and solving yields the disease-free equilibrium point

$E^0 = (S_p^0, A_p^0, I_p^0, R_p^0, S_s^0, A_s^0, I_s^0, I_h^0, R_s^0, V^0, S_v^0, I_v^0)=(\frac{\pi}{\mu}, 0, 0, 0, 0, 0, 0, 0, 0, 0, 0, \frac{B_v}{\mu_v}, 0)$.

4.2. The basic reproduction number

In a bid to establish the stability of the equilibrium, we will compute the basic reproduction number by adopting a technique known as the next-generation matrix method developed by [18].

Definition. The basic reproduction number is the number of secondary infections that result from a single infectious individual or mosquito when they are introduced into a wholly susceptible population [19].

Using Model 2.1, we divide the classes into diseased classes and non-diseased classes from which we get the matrix of new infections and the matrix of transitions represented by F and V, respectively, and evaluate their Jacobian at the disease-free equilibrium. Thus we have the following:

$$F = \begin{pmatrix} \theta\lambda_p S_p \\ \rho\lambda_p S_p \\ \theta\lambda_s S_s \\ \rho\lambda_s S_s \\ 0 \\ \lambda_v S_v \end{pmatrix}$$

Finding partial derivatives and evaluating the matrix F at the disease-free equilibrium, we obtain

$$F = \begin{pmatrix} 0 & 0 & 0 & 0 & 0 & \frac{\theta b\beta_{hp} S_p^0}{N_h} \\ 0 & 0 & 0 & 0 & 0 & \frac{\rho b\beta_{hp} S_p^0}{N_h} \\ 0 & 0 & 0 & 0 & 0 & 0 \\ 0 & 0 & 0 & 0 & 0 & 0 \\ 0 & 0 & 0 & 0 & 0 & 0 \\ \frac{b\eta\beta_{vp} S_v^0}{N_h} & \frac{b\beta_{vp} S_v^0}{N_h} & \frac{b\eta\beta_{sv} S_v^0}{N_h} & \frac{b\beta_{sv} S_v^0}{N_h} & 0 & 0 \end{pmatrix}$$

The following illustrates the derivations of the matrix of transitions

$$V = V^- - V^+ = \begin{pmatrix} \pi_1 A_p \\ \pi_2 I_p \\ \pi_3 A_s \\ \pi_4 I_s \\ \pi_5 I_h - \delta I_s \\ \pi_6 I_v \end{pmatrix}.$$

Again, finding partial derivatives and evaluating the Jacobian of V at disease-free equilibrium yields

$$V = \begin{pmatrix} \pi_1 & 0 & 0 & 0 & 0 & 0 \\ 0 & \pi_2 & 0 & 0 & 0 & 0 \\ 0 & 0 & \pi_3 & 0 & 0 & 0 \\ 0 & 0 & 0 & \pi_4 & 0 & 0 \\ 0 & 0 & 0 & -\delta & \pi_5 & 0 \\ 0 & 0 & 0 & 0 & 0 & \pi_6 \end{pmatrix},$$

where

$\pi_1 = \mu + \gamma, \pi_2 = \mu + \sigma, \pi_3 = \mu + \gamma, \pi_4 = \mu + \alpha + \delta, \pi_5 = \mu + \epsilon + d, \pi_6 = \mu_v.$

hus the matrix FV^{-1} is given as shown below:

$$FV^{-1} = \begin{pmatrix} 0 & 0 & 0 & 0 & 0 & \frac{b\theta\beta_h S_p^0}{N_h\mu_v} \\ 0 & 0 & 0 & 0 & 0 & \frac{b\rho\beta_h S_p^0}{N_h\mu_v} \\ 0 & 0 & 0 & 0 & 0 & 0 \\ 0 & 0 & 0 & 0 & 0 & 0 \\ 0 & 0 & 0 & 0 & 0 & 0 \\ \frac{b\eta\beta_{pv}S_v^0}{N_h(\mu+\gamma)} & \frac{b\beta_{pv}S_v^0}{N_h(\mu+\sigma)} & \frac{b\eta\beta_{vs}S_v^0}{N_h(\mu+\gamma)} & \frac{b\beta_{vs}S_v^0}{N_h(\mu+\alpha+\delta)} & 0 & 0 \end{pmatrix}.$$

Computing the eigenvalues for the above matrix we get

$$\left\{0, 0, 0, 0, -\frac{b}{N_h}\sqrt{\frac{\beta_{pv}\beta_{hp}S_v^0 S_p^0[\rho(\mu+\gamma)+\eta\theta(\mu+\sigma)]}{\mu_v(\mu+\gamma)(\mu+\sigma)}}, \frac{b}{N_h}\sqrt{\frac{\beta_{pv}\beta_{hp}S_v^0 S_p^0[\rho(\mu+\gamma)+\eta\theta(\mu+\sigma)]}{\mu_v(\mu+\gamma)(\mu+\sigma)}}\right\}.$$

The basic reproduction number is then obtained from the spectral radius of $\rho(FV^{-1})$ of the matrix FV^{-1}, defined as the largest absolute value of the eigenvalues of the matrix FV^{-1} when we study the

dynamics of the disease in the absence of control measures and is given as

$$R_0 = \frac{b}{N_h}\sqrt{\frac{\beta_{pv}\beta_{hp}S_v^0 S_p^0[\rho(\mu+\gamma)+\eta\theta(\mu+\sigma)]}{\mu_v(\mu+\gamma)(\mu+\sigma)}}.$$

In the absence of the disease, the values of S_p^0 and S_v^0 are known at disease-free equilibrium. Thus in parameter terms the basic reproduction number, R_0 is given by

$$R_0 = \sqrt{\frac{b^2\mu\beta_{hp}\beta_{vp}B_v[\rho(\mu+\gamma)+\eta\theta(\mu+\sigma)]}{\pi\mu_v^2(\mu+\gamma)(\mu+\sigma)}}.$$

4.3. Local stability analysis of the disease-free equilibrium point

Theorem 4.1. *The dengue fever-free equilibrium point of the system is locally asymptotically stable if* $R_0 < 1$*: otherwise, it is unstable.*

Proof. The disease-free equilibrium point E^0 is locally asymptotically stable if all the eigenvalues of the Jacobian matrix below evaluated at $J(E^0)$ are all negative or have negative real parts according to the Routh-Hurwitz criterion. Evaluating at $J(E^0)$ yields

$$J(E^0) = \begin{pmatrix}
-\mu & 0 & 0 & 0 & 0 & 0 & 0 & 0 & 0 & 0 & 0 & B^* \\
0 & -(\mu+\gamma) & 0 & 0 & 0 & 0 & 0 & 0 & 0 & 0 & 0 & D^* \\
0 & 0 & -(\mu+\sigma) & 0 & 0 & 0 & 0 & 0 & 0 & 0 & 0 & F^* \\
0 & \gamma & \sigma & -(\mu+\nu) & 0 & 0 & 0 & 0 & 0 & 0 & 0 & 0 \\
0 & 0 & 0 & 0 & -\mu & 0 & 0 & 0 & 0 & 0 & 0 & 0 \\
0 & 0 & 0 & 0 & 0 & -(\mu+\sigma) & 0 & 0 & 0 & 0 & 0 & 0 \\
0 & 0 & 0 & 0 & 0 & 0 & -(\mu+\alpha+\delta) & 0 & 0 & 0 & 0 & 0 \\
0 & 0 & 0 & 0 & 0 & 0 & \gamma & -(\mu+\epsilon+d) & 0 & 0 & 0 & 0 \\
0 & 0 & 0 & 0 & 0 & \gamma & \alpha & \epsilon & -\mu & 0 & 0 & 0 \\
0 & 0 & 0 & \omega & 0 & 0 & 0 & 0 & 0 & -(\mu+\kappa) & 0 & 0 \\
0 & M^* & N^* & 0 & 0 & W^* & P^* & 0 & 0 & 0 & -\mu_v & 0 \\
0 & Q^* & R^* & 0 & 0 & S^* & T^* & 0 & 0 & 0 & 0 & -\mu_v
\end{pmatrix}$$

To assess the nature of the eigenvalues, we deduce the characteristic polynomial of the Jacobian matrix evaluated at E^0 using the equation $|J(E^0) - \lambda I| = 0$ with asterisked unknowns defined in Supplementary Material.

The characteristic equation for the matrix above is given by

$$(-\lambda-\mu)^3(-\gamma-\lambda-\mu)(-\gamma-\delta-\lambda-\mu)(-d-\epsilon-\lambda-\mu)(-\kappa-\lambda-\mu)(-\lambda-\mu-\nu)(-\lambda-\mu_v)\Pi = 0$$

The eigenvalues of the matrix J are given as follows:

$$\begin{cases} \lambda_1 = -\mu \\ \lambda_2 = -\mu \\ \lambda_3 = -\mu \\ \lambda_4 = -\mu_v \\ \lambda_5 = -(\gamma+\mu) \\ \lambda_6 = -(\mu+\kappa) \\ \lambda_7 = -(\mu+\nu) \\ \lambda_8 = -(\gamma+\delta+\mu) \\ \lambda_9 = -(d+\epsilon+\mu), \end{cases} \tag{4.1}$$

where

$$\Pi = -\lambda^3 - \lambda^2(\gamma+\sigma+2\mu+\mu_v) + \lambda\left(\sqrt{\frac{b^2\mu B_v\beta_{hp}\beta_{vp}(\eta\theta+\rho)}{\pi\mu_v[(\gamma+\mu)(\mu+\sigma)+\mu_v(\gamma+\sigma+2\mu)]}} - 1\right) + \left(\sqrt{\frac{b^2\mu\beta_{hp}\beta_{vp}B_v[\rho(\mu+\gamma)+\eta\theta(\mu+\sigma)]}{\pi\mu_v(\mu+\gamma)(\mu+\sigma)}} - 1\right) = 0$$

Rewriting the characteristic polynomial Π in terms of the basic reproduction number, we have

$$\Pi = P(\lambda) = -\lambda^3 - \lambda^2(\gamma+\sigma+2\mu+\mu_v) + \lambda(R_c^2 - 1) + (R_0^2 - 1) = 0,$$

where R_c^2 and R_0^2 are given as

$$R_c = \sqrt{\frac{b^2\mu B_v\beta_{hp}\beta_{vp}(\eta\theta+\rho)}{\pi\mu_v[(\gamma+\mu)(\mu+\sigma)+\mu_v(\gamma+\sigma+2\mu)]}} \quad \text{and} \quad R_0 = \sqrt{\frac{b^2\mu\beta_{hp}\beta_{vp}B_v[\rho(\mu+\gamma)+\eta\theta(\mu+\sigma)]}{\pi\mu_v^2(\mu+\gamma)(\mu+\sigma)}}.$$

4.4. Relationship between R_0 and R_c

We compute the ratio $\dfrac{R_c^2}{R_0^2}$ as follows:

$$\frac{R_c}{R_0} = \sqrt{\frac{\mu_v(\eta\theta+\rho)(\mu+\gamma)(\mu+\sigma)}{[(\mu+\gamma)(\mu+\sigma)+\mu_v(\gamma+\sigma+2\mu)][\rho(\mu+\gamma)+\eta\theta(\mu+\sigma)]}}. \tag{4.2}$$

The relationship above shows that R_c is a scaled multiple of the basic reproduction number R_0 with a scaling factor

$$k = \sqrt{\frac{\mu_v(\eta\theta+\rho)(\mu+\gamma)(\mu+\sigma)}{[(\mu+\gamma)(\mu+\sigma)+\mu_v(\gamma+\sigma+2\mu)][\rho(\mu+\gamma)+\eta\theta(\mu+\sigma)]}}. \tag{4.3}$$

To investigate the magnitude of the scaling factor k, we subtract the numerator from the denominator as follows:

$$[(\mu+\gamma)(\mu+\sigma)+\mu_v(\gamma+\sigma+2\mu)][\rho(\mu+\gamma)+\eta\theta(\mu+\sigma)] - \mu_v(\eta\theta+\rho)(\mu+\gamma)(\mu+\sigma) > 0, \tag{4.4}$$

and we get the following expression:

$$[(\gamma+\mu)(\mu+\sigma)][\rho(\gamma+\mu)+\eta\theta(\mu+\sigma)]+\mu_v[\rho(\gamma+\mu)^2+\eta\theta(\mu+\sigma)^2]>0, \tag{4.5}$$

which shows that the denominator is always greater than the numerator, and thus the scaling factor is always $k < 1$, and this suggests that $R_c < R_0$ given that for Model 2.1, the parameters are always positive. The assertion above is numerically verified for Model 2.1 as evidenced by Figure 2 using the parameter values from Table 4.

For simplicity, we multiply the characteristic polynomial by -1 and analyze the resulting polynomial using the Routh-Hurwitz criterion;

$$\Pi = P(\lambda) = a_0\lambda^3 + a_1\lambda^2 + \lambda(1-R_0^2k) + (1-R_0^2) = 0, \tag{4.6}$$

where $a_0 = 1$, $a_1 = (\gamma+\sigma+2\mu+\mu_v)$, $a_2 = (1-R_0^2k)$ and $a_3 = (1-R_0^2)$

Thus, by the Routh-Hurwitz criterion outlined in Matcheva [20], for a third-degree polynomial, it suffices to say that all roots of the characteristic polynomial are located in the open left half-plane for $R_0 < 1$ given that $a_1a_2 > a_3$.

Thus considering that all the other eigenvalues for the system are negative, it implies that the DFE point is locally asymptotically stable. □

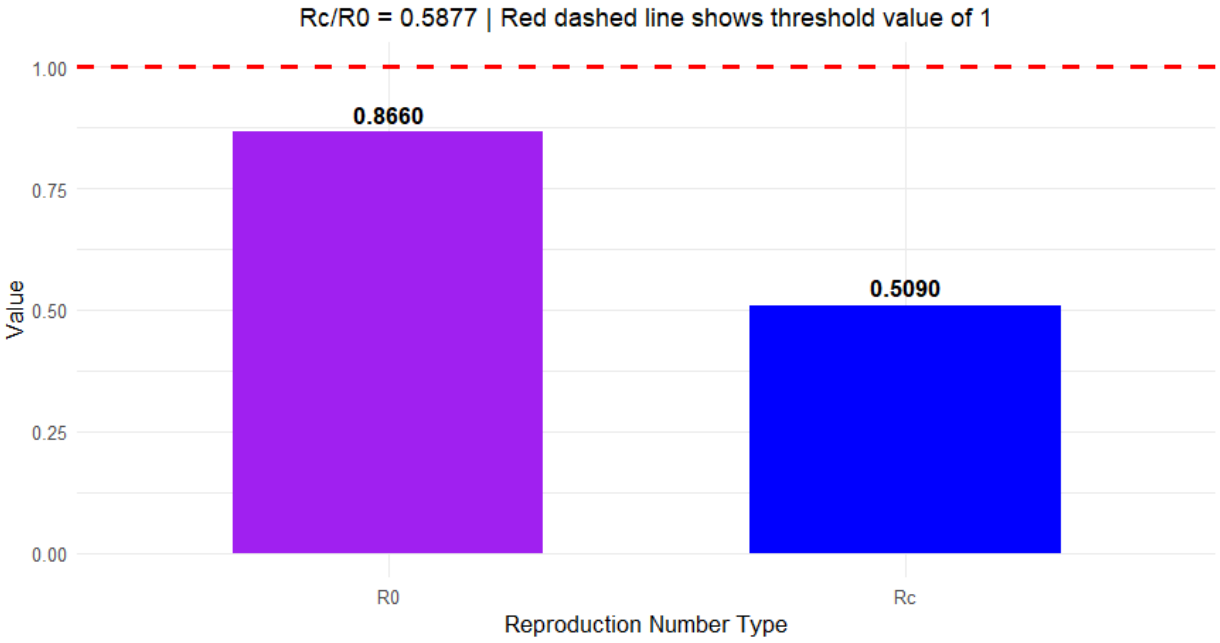

Figure 2. Comparison of R_c and R_0.

5. Existence of the endemic equilibrium point

5.1. Case 1: Primary infection dynamics

Considering the reduced model governing the primary infection dynamics, the existence of an endemic equilibrium point (EEP) is established and rigorously demonstrated. The formal proof of existence is provided in the Supplementary Material, and the principal findings are summarized in the following theorem.

Theorem 5.1. *Considering the primary infection dynamics, the model will admit the following equilibria:*

1. *The DFE exists whenever* $R_0 \leq 1$.
2. *The EEP exists and is unique if and only if* $R_0 > 1$.

This clearly shows that for primary infection dynamics with no disease-induced death, the system will only exhibit forward bifurcation.

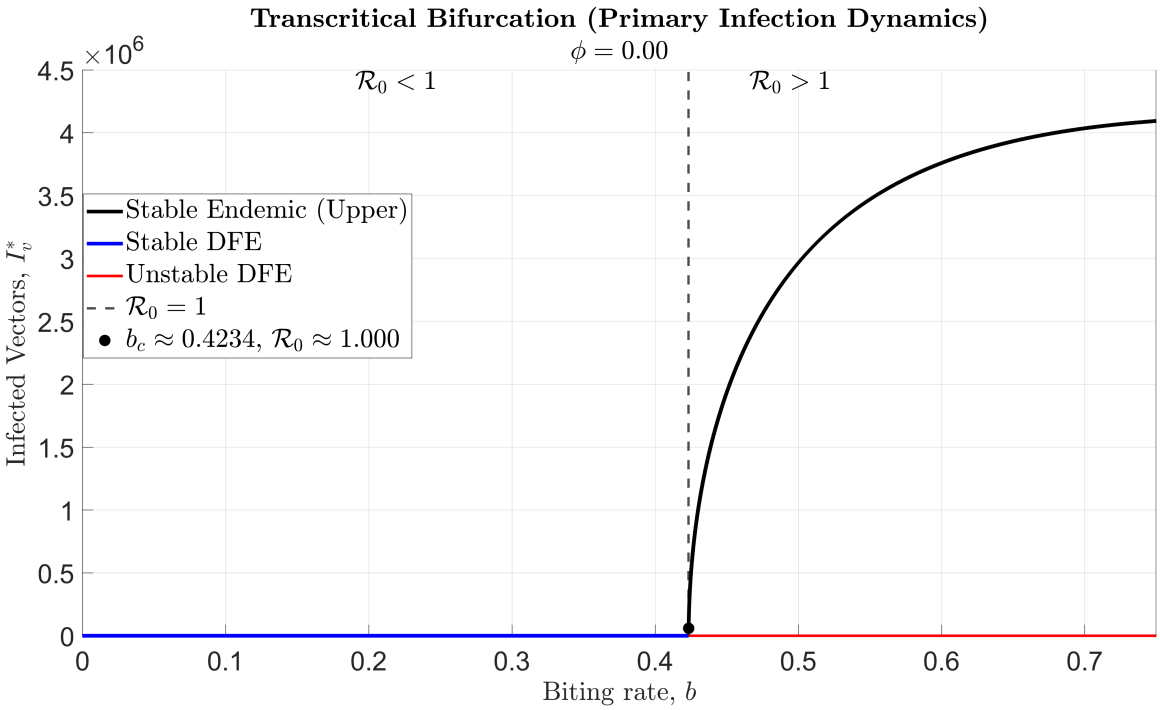

Figure 3. Transcritical bifurcation diagram for primary infection dynamics.

In the limiting case where ADE is absent (i.e. $\phi = 0$), numerical simulations demonstrate that disease transmission is entirely driven by primary infection pathways, as secondary infection mechanisms and waning immunity exert no influence whatsoever on the overall transmission dynamics. Notably, when the mosquito biting rate b is taken as the bifurcation parameter, the model undergoes a transcritical bifurcation at $\mathcal{R}_0 = 1$ at the threshold $b_c \approx 0.4234$. For values of $b > b_c$, the system transitions to a stable endemic equilibrium point (EEP), accompanied by a marked increase in the infection bur-

den within the host population. This result underscores the pivotal role of the mosquito biting rate in sustaining the infection's endemicity and amplifying disease prevalence. Consequently, these findings highlight the necessity of targeted public health interventions directed at reducing mosquito-to-host transmission, including sustained vaccination campaigns, personal protective measures, rigorous long-term disease surveillance programmes, and integrated vector control strategies.

5.2. Case 2: Assuming negligible deaths in overall disease dynamics

We now examine the infection dynamics of the complete model and establish the existence of an EEP through the derivation of a characteristic polynomial. See Supplementary Material for full derivation. The polynomial has the coefficients A_0, A_1, and A_2, analogous to

$$\lambda_p^*(A_0\lambda_p^{*2} + A_1\lambda_p^* + A_2) = 0. \tag{5.1}$$

It is known that $\lambda_p^* = 0$ is a trivial solution corresponding to the disease-free equilibrium, so thus at the endemic equilibrium point we have two non-trivial solutions that are solutions of the polynomial

$$A_0\lambda_p^{*2} + A_1\lambda_p^* + A_2 = 0, \tag{5.2}$$

that are given by

$$\lambda_{p(1,2)}^* = \frac{-A_1 \pm \sqrt{A_1^2 - 4A_0A_2}}{2A_0}. \tag{5.3}$$

For Equation 5.2 to have at least one unique positive root, we will use Descartes' rule of signs [21] to assess the existence of real roots and we summarize the results in Table 3.

Table 3. Possible count of positive roots.

Case	A_0	A_1	A_2	R_0	Number of roots
1	+	+	+	< 1	0
2	+	−	+	< 1	0, 2
3	+	−	−	> 1	1
4	+	+	−	> 1	1

These results indicate the possibility of a backward bifurcation, as seen by the presence of two equilibria when $R_0 < 1$. We therefore summarize the observed conclusions in the following theorem.

Theorem 5.2. *The system will admit the following equilibria:*

1. *There is no positive root when Case* 1 *holds implying only the DFE will exist.*
2. *The system will exhibit backward bifurcation when Case* 2 *holds.*
3. *The system will exhibit a unique EEP regardless of the sign of* A_1 *when Cases* 3 *and* 4 *hold.*

The theorem above necessitates a bifurcation analysis as described in the bifurcation analysis section; however, we first need to establish the disease's persistence within the population.

6. Global stability analysis of the endemic equilibrium point

The endemic equilibrium point (EEP) of the proposed model is demonstrated to be globally asymptotically stable, with a detailed proof presented in the Supplementary Material.

7. Bifurcation analysis

For the given dynamical system, a bifurcation analysis is rigorously carried out, with a detailed proof provided in the Supplementary Material, and the principal result is stated in the following theorem.

Theorem 7.1. *Following the bifurcation analysis,*

1. *When $a > 0$, meaning that when*

$$\left[\frac{\eta\theta N_h S_v v_{12}(\nu(1-\omega)w_4+w_{10}\kappa)\beta_{hs}\beta_{vs}\mu_v(\theta(\alpha+\delta+\mu)+\rho(\sigma+\mu))}{\mu(\alpha+\delta+\mu))(\sigma+\mu)}\right] > \left[\frac{b\theta(\gamma+\mu+\eta(\delta+\mu))S_p^2(\theta v_2+\rho v_3)w_{12}\beta_{hp}^2\beta_{hs}}{(\gamma+\mu)(\delta+\mu)} + \frac{bS_pS_v v_{12}w_{12}\beta_{hp}^2\beta_{vp}\mu_v(\rho(\gamma+\mu)+\eta\theta(\sigma+\mu))}{\mu(\gamma+\mu)(\sigma+\mu)}\right],$$

the system will undergo backward bifurcation when $R_0 = 1$ and $\beta_{hp} = \beta_{hp}^*$.

2. *When $a < 0$, meaning that when*

$$\left[\frac{\eta\theta N_h S_v v_{12}(\nu(1-\omega)w_4+w_{10}\kappa)\beta_{hs}\beta_{vs}\mu_v(\theta(\alpha+\delta+\mu)+\rho(\sigma+\mu))}{\mu(\alpha+\delta+\mu))(\sigma+\mu)}\right] < \left[\frac{b\theta(\gamma+\mu+\eta(\delta+\mu))S_p^2(\theta v_2+\rho v_3)w_{12}\beta_{hp}^2\beta_{hs}}{(\gamma+\mu)(\delta+\mu)} + \frac{bS_pS_v v_{12}w_{12}\beta_{hp}^2\beta_{vp}\mu_v(\rho(\gamma+\mu)+\eta\theta(\sigma+\mu))}{\mu(\gamma+\mu)(\sigma+\mu)}\right],$$

the system will undergo forward bifurcation when $R_0 = 1$ and $\beta_{hp} = \beta_{hp}^*$.

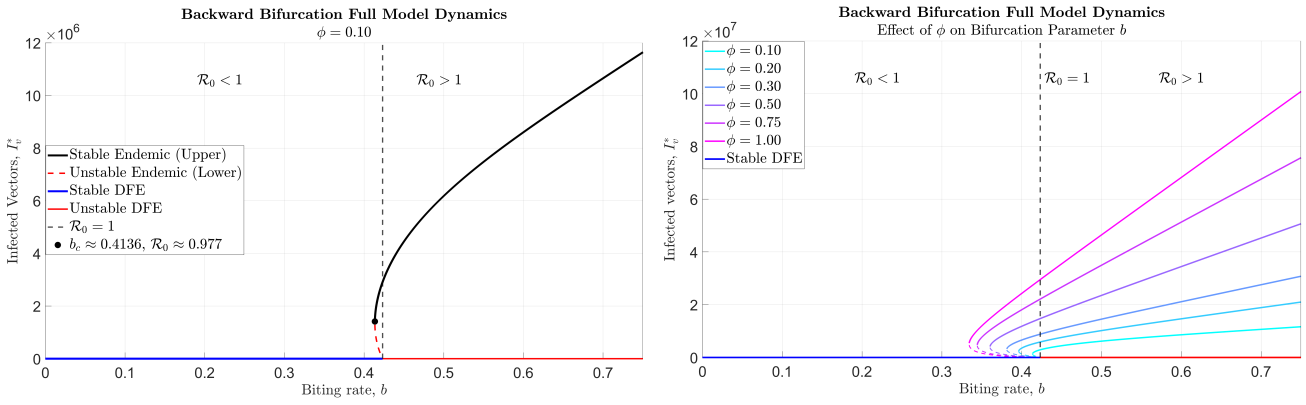

(a) Bifurcation due to b at $\phi = 0.10$ (b) Bifurcation due to b as ϕ increases

Figure 4. Backward bifurcation due to b.

Figure 4(a), (b) further illustrates the existence of a backward bifurcation structure and its epidemiological implications. Notably, the same qualitative backward bifurcation is observed across all selected values of the ADE ϕ, confirming that backward bifurcation is a robust feature of the model.

As ADE ϕ increases, the critical biting rate b_c at which backward bifurcation occurs decreases, implying that higher ADE values ϕ expand the basin of attraction of the endemic equilibrium. The critical value of b at b_c marks the saddle-node bifurcation point where the two endemic branches meet, such that for $b < b_c$, the disease-free equilibrium is the only attractor. From an epidemiological standpoint, the bistable region $b \in [b_c, 0.42)$ represents the most critical zone, where the disease-free equilibrium (DFE) and the endemic equilibrium point (EEP) coexist for values of $\mathcal{R}_0 < 1$ and the disease persists, confirming that intervention strategies must reduce the biting rate sufficiently below a critical threshold b_c to guarantee disease eradication.

8. Robustness of bistability

When a system with backward bifurcation is bistable, it has a basin of attraction. One of the fundamental characteristics of backward bifurcation is the concept of robustness, which is a long-recognized hallmark in biological systems [22, 23]. For the backward bifurcation observed, we can define robustness as the ability of the system to maintain backward bifurcation under perturbations and uncertainty. Thus, on the basis of the backward bifurcation analysis and the definition of robustness of the bifurcation, we arrive at the following theorem.

Theorem 8.1. *If the robustness integral R is $R > 0$, then the developed Model 2.1 will exhibit a backward bifurcation.*

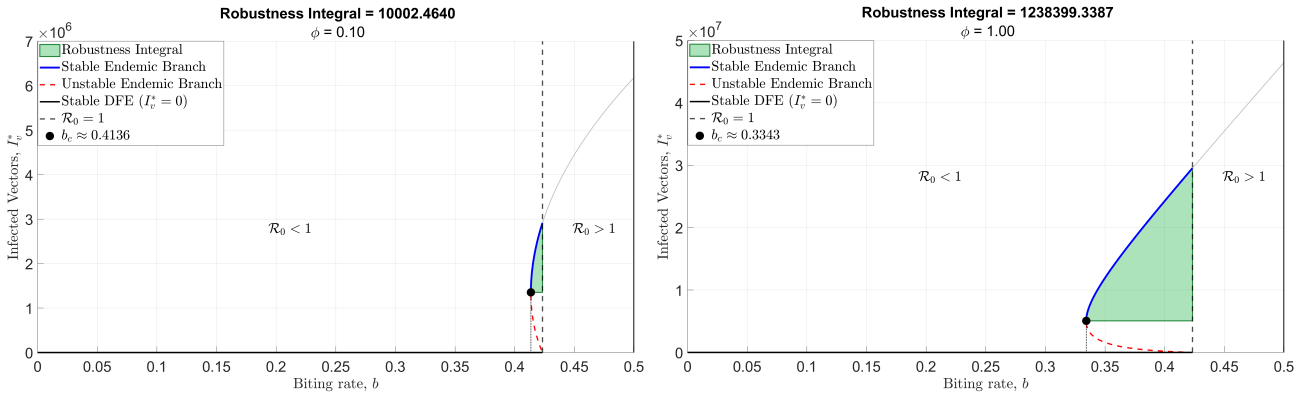

(a) Robustness of backward bifurcation at $\phi = 0.10$. (b) Robustness of backward bifurcation as ϕ increases to $\phi = 1.0$.

Figure 5. Robustness diagrams.

The robustness integral $I(\phi)$ measures how strongly the endemic equilibrium persists within the bistability window $[b_c, b^*]$ where $\mathcal{R}_0 < 1$. In the integral, ϕ denotes the Antibody-Dependent Enhancement (ADE), which paradoxically amplifies secondary infections rather than conferring immunity. As ϕ increases, so does $I(\phi)$, showing that high ADE values increase the region of endemic persistence below the epidemic threshold. When ADE is strong and $I(\phi)$ is large, reducing $\mathcal{R}_0$ below unity is necessary but insufficient for disease elimination. ADE-amplified secondary infections sustain transmission independently of the reproductive threshold, maintaining the system at the stable endemic equilibrium point across a wide bistability window. Thus, prior exposure to the infection becomes a

driver of secondary infections rather than protection, and any relaxation of the control measures risks a sharp rebound in infections. Critically, vaccinating seronegative individuals becomes detrimental, as partial immunity may raise the effective ϕ, worsening disease outcomes in seronegative populations. Disease elimination requires driving the biting rate below the saddle-node threshold b_c through sustained vector control measures, seropositive vaccination, and the use of protective measures such as insecticide-treated bed nets. When ADE is weak and $I(\phi)$ is small, the significance of the endemic equilibrium point within the bistability window is epidemiologically negligible, prior immunity maybe protective, and reducing $\mathcal{R}_0$ below 1 is sufficient for practical disease elimination with a lower risk of disease rebound.

9. Global stability analysis of the disease-free equilibrium point

Lemma 1. *The existence of a transcritical bifurcation in our model for $a < 0$ gives rise to a unique DFE which collides with a unique EEP giving rise to an exchange in stability when $\mathcal{R}_0$ transcends 1.*

The lemma above leads us to the following theorem.

Theorem 9.1. *The disease-free equilibrium point E^0 is globally asymptotically stable if $\mathcal{R}_0 < 1$; otherwise, it is unstable.*

Proof. To prove the global stability of the disease-free equilibrium point we use the concept of a quasi positive matrix also known as the Metzler matrix. We divide the given system of differential equations describing our model into transmitting and non transmitting components.

Let Y_1 be the vector for non-transmitting compartments and Y_2 be the vector for the transmitting compartments, and let E_0 be the vector denoting the disease-free equilibrium point.

$$\frac{dY_1}{dt} = \mathbf{A}_1(Y_1 - Y_1(E_0)) + \mathbf{A}_2 Y_2$$
$$\frac{dY_2}{dt} = \mathbf{A}_3 Y_2$$

where $Y_1 = (S_p, R_p, S_s, I_h, R_s, V, S_v)$ and $Y_1 = (A_p, I_p, A_s, I_s, I_v)$.

To prove the global stability of the disease-free equilibrium, we need to establish that the matrix A_1 has real eigenvalues that are negative and that the matrix A_3 is a Metzler matrix with non-negative off-diagonal elements.

Rewriting the presented dengue fever model, we get the following:

$$\begin{pmatrix} \pi - \lambda_p S_p - \mu S_p \\ \gamma A_p + \sigma I_p - (\mu + \nu) R_p \\ (1-\omega)\nu R_p + \kappa V - (\lambda_s + \mu) S_s \\ \delta I_s - (\mu + \epsilon + d) I_h \\ \gamma A_s + \alpha I_s + \epsilon I_h - \mu R_s \\ \omega \nu R_p - (\mu + \kappa) V \\ B_v - (\lambda_v + \mu_v) S_v \end{pmatrix} = \mathbf{A}_1 \begin{pmatrix} S_p - \frac{\pi}{\mu} \\ 0 \\ 0 \\ 0 \\ 0 \\ 0 \\ S_v - \frac{B_v}{\mu_v} \end{pmatrix} + \mathbf{A}_2 \begin{pmatrix} A_p \\ I_p \\ A_s \\ I_s \\ I_v \end{pmatrix}$$

and

$$\begin{pmatrix} \theta\lambda_1 S_p - (\mu+\gamma)A_p \\ \rho\lambda_1 S_p - (\mu+\sigma)I_p \\ \theta\lambda_s S_s - (\mu+\gamma)A_s \\ \rho\lambda_2 S_s - (\mu+\alpha+\delta)I_s \\ \lambda_v S_v - (\mu_v+\psi_v)I_v \end{pmatrix} = \mathbf{A}_3 \begin{pmatrix} A_p \\ I_p \\ A_s \\ I_s \\ I_v \end{pmatrix}.$$

Now, using the transmitting and non-transmitting classes of the model, we get the following matrices A_1, A_2, and A_3:

$$\mathbf{A}_1 = \begin{pmatrix} -\lambda_p - \mu & 0 & 0 & 0 & 0 & 0 & 0 \\ 0 & -(\mu+\nu) & 0 & 0 & 0 & 0 & 0 \\ 0 & (1-\omega) & -\lambda_s - \mu & 0 & 0 & \kappa & 0 \\ 0 & 0 & 0 & -(\mu+\epsilon+d) & 0 & 0 & 0 \\ 0 & 0 & 0 & \epsilon & -\mu & 0 & 0 \\ 0 & \omega & 0 & 0 & 0 & -(\mu+\kappa) & 0 \\ 0 & 0 & 0 & 0 & 0 & 0 & -\lambda_v - \mu_v \end{pmatrix}$$

$$\mathbf{A}_2 = \begin{pmatrix} 0 & 0 & 0 & 0 & \frac{-b\beta_{hp}}{N} \\ \gamma & \sigma & 0 & 0 & 0 \\ 0 & 0 & 0 & 0 & \frac{-b\beta_{hp}}{N} \\ 0 & 0 & 0 & \delta & 0 \\ 0 & 0 & \gamma & \alpha & 0 \\ 0 & 0 & 0 & 0 & 0 \\ \frac{-b\beta_{vp}\eta S_v}{N_h} & \frac{-b\beta_{vp} S_v}{N_h} & \frac{-b\beta_{vs} S_v}{N_h} & \frac{-b\beta_{vs} S_v}{N_h} & 0 \end{pmatrix}$$

and

$$\mathbf{A}_3 = \begin{pmatrix} -(\mu+\gamma) & 0 & 0 & 0 & 0 \\ 0 & -(\mu+\gamma) & 0 & 0 & 0 \\ 0 & 0 & -(\mu+\delta) & 0 & 0 \\ 0 & 0 & 0 & -(\mu+\alpha+\delta) & 0 \\ \frac{b\beta_{vp}\eta S_v}{N_h} & \frac{b\beta_{vp} S_v}{N_h} & \frac{b\beta_{vs} S_v}{N_h} & \frac{b\beta_{vs} S_v}{N_h} & -\mu_v \end{pmatrix}.$$

Taking into consideration the matrix A_1, we observe, via computation, that the matrix has real and negative eigenvalues which proves that the dengue fever system in the form

$$\frac{dY_1}{dt} = \mathbf{A}_1(Y_1 - Y_1(E_0)) + \mathbf{A}_2 Y_2,$$

is globally and asymptotically stable at the disease-free equilibrium point; that is, when $\mathcal{R}_0 < 1$. Considering the matrix A_3, it is evident that the off-diagonal elements of the matrix are all non-negative which implies that the matrix is Metzler stable. This establishes that the disease-free equilibrium point is globally asymptotically stable when $\mathcal{R}_0 < 1$; otherwise, it is unstable. □

10. Main results

10.1. Sensitivity analysis

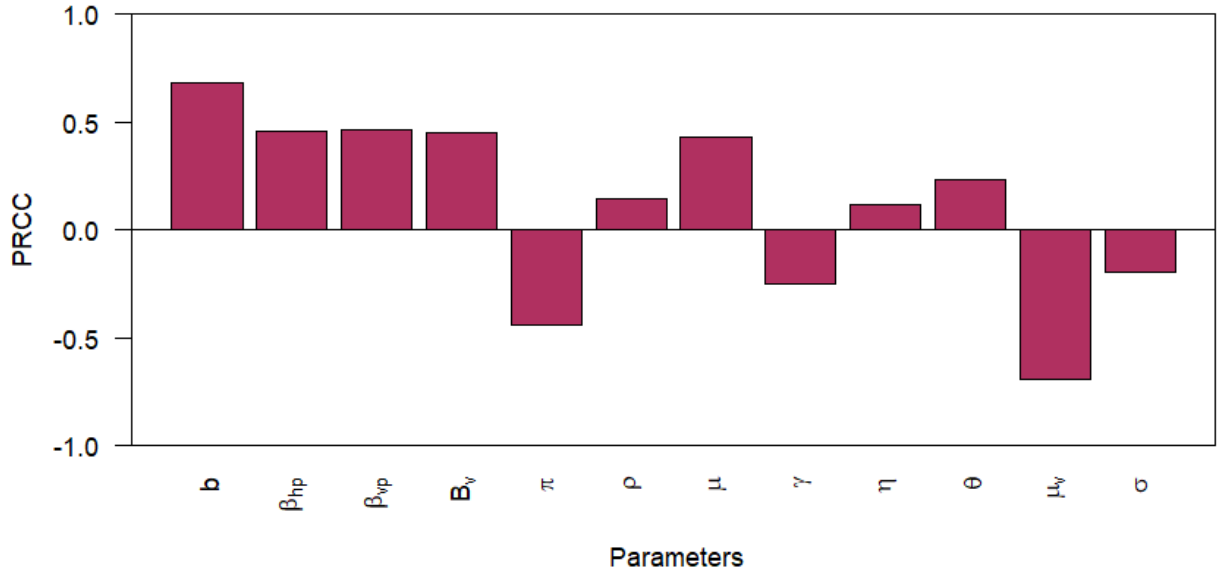

Figure 6. Tornado plot for the sensitivity analysis.

Effective mitigation of disease transmission necessitates the systematic identification of the parameters that exert the greatest influence on the epidemic's dynamics. To rigorously quantify the relative contribution of each model parameter to the transmission of dengue fever, a global sensitivity analysis was conducted with the basic reproduction number, $\mathcal{R}_0$, as the response function. The basic reproduction number constitutes a fundamental epidemiological threshold metric governing the dynamics of infectious disease transmission. Given the inherent constraints on the resources available for dengue fever control interventions, this analysis facilitates the identification of parameters with a disproportionate influence on disease propagation, thereby enabling the strategic allocation of targeted control measures toward those parameters of greatest epidemiological significance.

In this section, the Latin hypercube sampling (LHS) scheme is used to perform the global sensitivity analysis. This method requires the specification of a baseline value and a corresponding range for each parameter under consideration. All parameters incorporated into the response function are assumed to conform to a uniform probability distribution. The relative impact of each parameter on the response function is assessed through the sign and magnitude of the partial rank correlation coefficient (PRCC). Parameters yielding negative PRCC values are associated with a reduction in disease transmissibility, whereas those exhibiting positive PRCC values are indicative of enhanced propagation of

the epidemic.

10.2. Numerical simulations

Numerical simulations of the developed mathematical model were implemented in MATLAB and R-Studio, with the parameter values used in the simulations presented in Table 4. Figure 7 illustrates the long-term temporal dynamics of both primary and secondary infections under the baseline conditions. The subsequent figures demonstrate the disease dynamics under reduced values of the per capita transmission rate of primary infection from vector to host, β_{hp}, and the mosquito biting rate, b, to levels sufficient to render the basic reproduction number $\mathcal{R}_0$ below the critical threshold of unity. Within the framework of epidemiological modeling, the condition $\mathcal{R}_0 < 1$ corresponds to disease-free equilibrium, a state in which the number of secondary infections generated by an initial primary infection diminishes monotonically over time, ultimately culminating in disease eradication.

Through the sensitivity analysis of the basic reproduction number $\mathcal{R}_0$, the parameters β_{hp}, β_{vp}, and B_v (with PRCC values marginally below 0.5) and π (with a PRCC value marginally exceeding -0.5) are identified as statistically significant determinants of disease dynamics. The epidemiological implications of these findings are evidenced by the tornado plot generated from the global sensitivity analysis of $\mathcal{R}_0$, wherein an incremental increase in parameters exerting a positive influence on $\mathcal{R}_0$ precipitates enhanced disease propagation and promotes the persistence of infection within the population. Conversely, a reduction in each of these parameter values produces a corresponding decrease in $\mathcal{R}_0$. Provided that $\mathcal{R}_0 < 1$, this condition constitutes a necessary criterion for the elimination of the disease from the population.

In the preceding model analysis, numerical evidence suggested the potential existence of backward bifurcation, which was analytically demonstrated to be contingent upon the sign of the bifurcation coefficient a. It was established that values of $a < 0$ give rise to forward bifurcation in the system. The epidemiological consequence of $a < 0$ is that the disease-free equilibrium represents the unique equilibrium state when $\mathcal{R}_0 < 1$, as formally established in Theorem 5.2, Case 1. Under this condition, $\mathcal{R}_0 < 1$ constitutes not merely a necessary but also a sufficient condition for disease eradication. Furthermore, as corroborated by Theorem 5.2, Cases 3 and 4, for $\mathcal{R}_0 > 1$, a unique EEP is guaranteed to exist irrespective of the sign of the coefficient A_1. See Supplementary Material.

For values of $a > 0$, the system is demonstrated to exhibit backward bifurcation, a phenomenon substantiated by Theorem 5.2, Case 2, in which the coexistence of two stable equilibria is rigorously established for $\mathcal{R}_0 < 1$. The epidemiological implications of this phenomenon are of considerable significance: In the presence of backward bifurcation, the condition $\mathcal{R}_0 < 1$ is reduced to a necessary but insufficient condition for disease eradication. Specifically, the successful elimination of the disease requires that the implemented control measures suppress $\mathcal{R}_0$ below a more stringent critical threshold, $\mathcal{R}_c$ associated with b_c, beyond which disease eradication can be guaranteed. This implies that conventional control strategies targeting $\mathcal{R}_0 < 1$ may prove inadequate in the presence of backward bifurcation, necessitating more aggressive and sustained intervention efforts to drive the system below the subcritical threshold $\mathcal{R}_c$ required for definitive disease elimination.

Table 4. Model parameter values.

Parameter	Value	Source
π	45	Assumed
μ	0.00004566	[24]
γ	0.146	[25]
ρ	(0.0-1.0)	Varies
α	0.04761	[26, 27]
σ	0.07146	[26, 27]
ϵ	0.062	Assumed
η	(1.0 – 3.0)	Varies
ω	(0.0-1.0)	Varies
ν	0.0177	[28]
ϕ	[0.0-1.0]	Varies
θ	(0.0-1.0)	[28]
b	0.50	[29]
d	0.01	[30]
B_v	500000	Assumed
κ	0.000578	[31]
δ	0.0714	Assumed
μ_v	0.09523	[32]
β_{hp}	0.19	[32]
β_{vp}	0.20	[32]
β_{hs}	0.85	[33]
β_{vs}	0.85	[33]

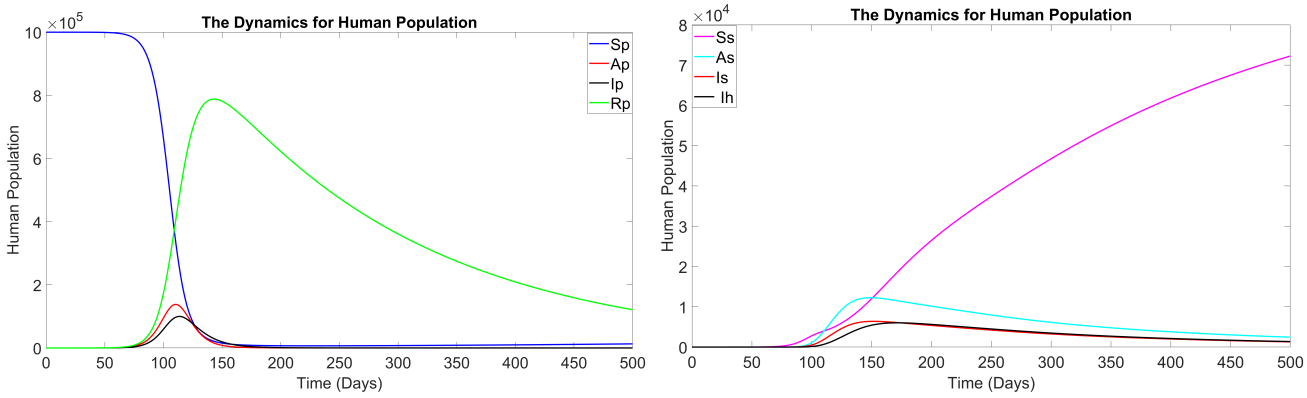

(a) Primary infection dynamics

(b) Secondary infection dynamics

Figure 7. Numerical simulations of the long-term dynamics of dengue fever.

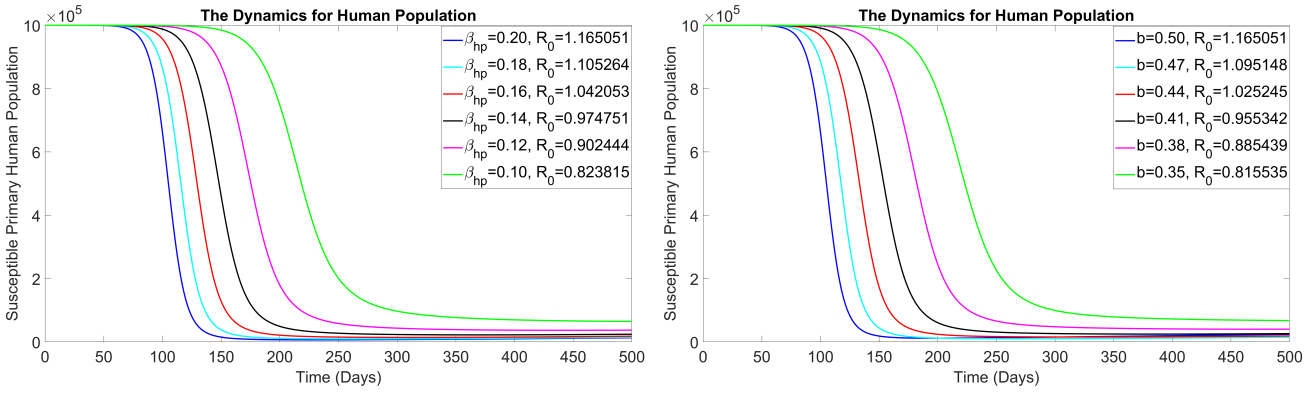

(a) (b)

Figure 8. Effects of β_{hp} and the biting rate b on the susceptible primary human population.

Figure 7(a) illustrates the temporal dynamics of primary dengue fever infections at the onset of the epidemic and the corresponding long-term evolution of the associated population compartments. The initial decline observed in the susceptible primary human population is associated with a progressive increase in the asymptomatic and symptomatic infection compartments, as well as the recovered primary population, reflecting the initial invasion and subsequent propagation of the disease through the susceptible host population.

Figure 7(b) depicts the temporal dynamics of secondary dengue fever infections as the epidemic progresses. As individuals recover from the primary infection, a notable temporal delay is observed in the emergence of secondary infection dynamics, attributable to the transient cross-immunity conferred upon recovery from the primary infection. This delay is further corroborated by the asynchronous attainment of peak values in the primary and secondary infection compartments, which occur at distinctly different time intervals, underscoring the sequential and immunologically mediated nature of the transition between primary and secondary infection dynamics.

Figure 8(a), (b) illustrates the dynamics of the susceptible primary population due to changes in the per capita transmission rate and the mosquito biting rate, respectively. Figure 8(a) demonstrates that a progressive reduction in the per capita transmission rate corresponds to a decline in the basic reproduction number $\mathcal{R}_0$, thereby reducing the rate of disease propagation within the host population. Figure 8(b) reveals analogous dynamics, wherein a systematic reduction in the mosquito biting rate is sufficient to suppress $\mathcal{R}_0$ below the critical threshold of unity, resulting in a substantial deceleration of disease transmission and progression toward epidemic control.

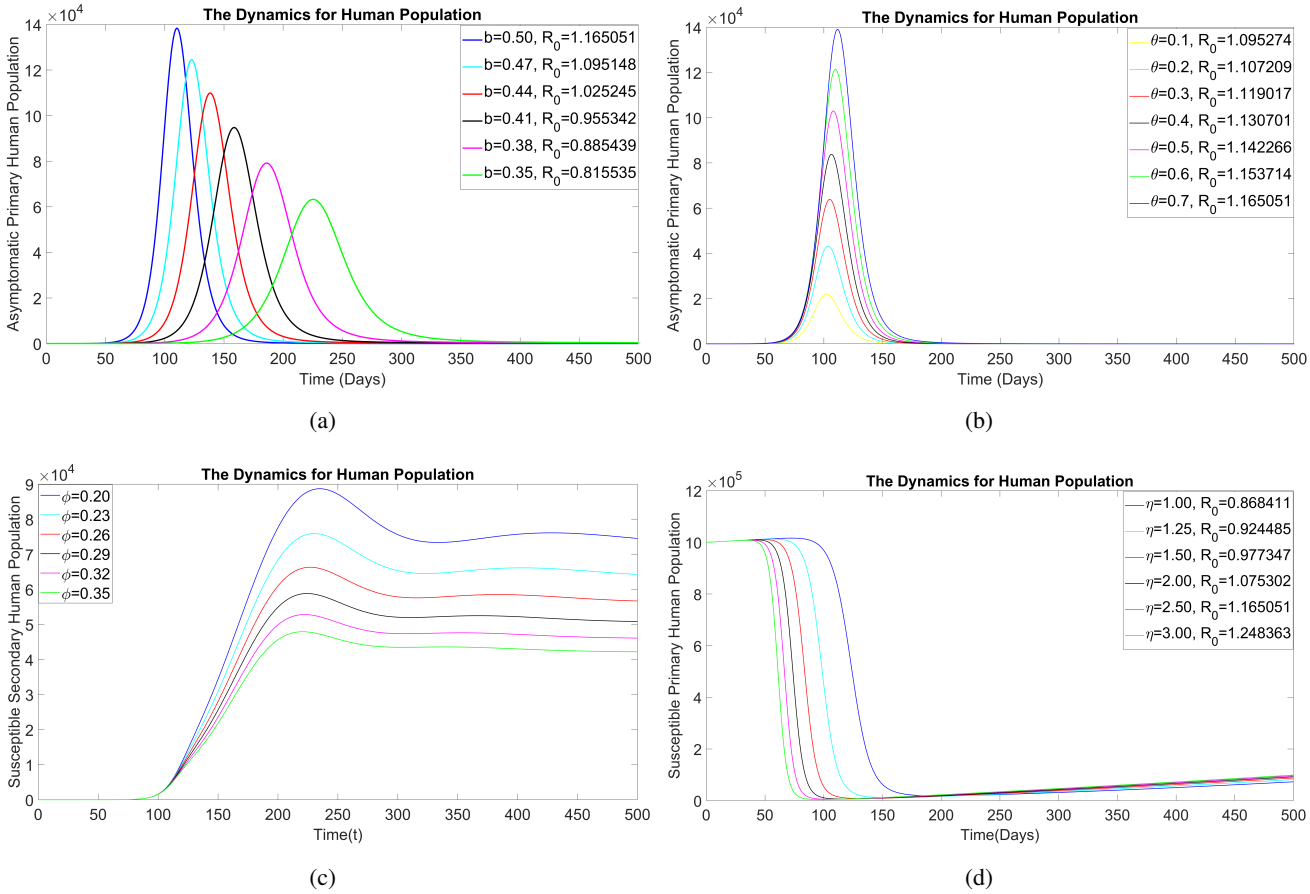

Figure 9. Effects of b, θ, ϕ, and η on the human population.

Figure 9(a) illustrates the temporal evolution of the asymptomatic primary human population compartment as a function of varying mosquito biting rates, demonstrating the sensitivity of asymptomatic primary infection dynamics to perturbations in this key entomological parameter.

Figure 9(b) demonstrates that the presence of asymptomatic infections exerts a significant influence on the overall transmission dynamics of dengue fever, wherein both elevated and diminished levels of asymptomatic infections' prevalence contribute to the establishment and maintenance of disease endemicity within the host population.

Figure 9(c) reveals that progressive increments in the ADE parameter ϕ precipitate substantial changes in the susceptible secondary human population compartment, S_s, attributable to the modulatory effect of ϕ on the secondary force of infection λ_s. This observation underscores the mechanistic role of ADE in amplifying secondary infections' dynamics by augmenting the susceptibility of previously infected individuals to subsequent heterologous serotype infections.

Figure 9(d) illustrates the effect of variations in the asymptomatic modification parameter η on the susceptible primary human population compartment, S_p. The results demonstrate that elevated values of η exert a pronounced destabilizing effect on the susceptible primary population, thereby promoting conditions conducive to disease endemicity. This highlights the epidemiological significance of asymptomatic transmission as a critical in sustaining dengue fever's persistence within the population.

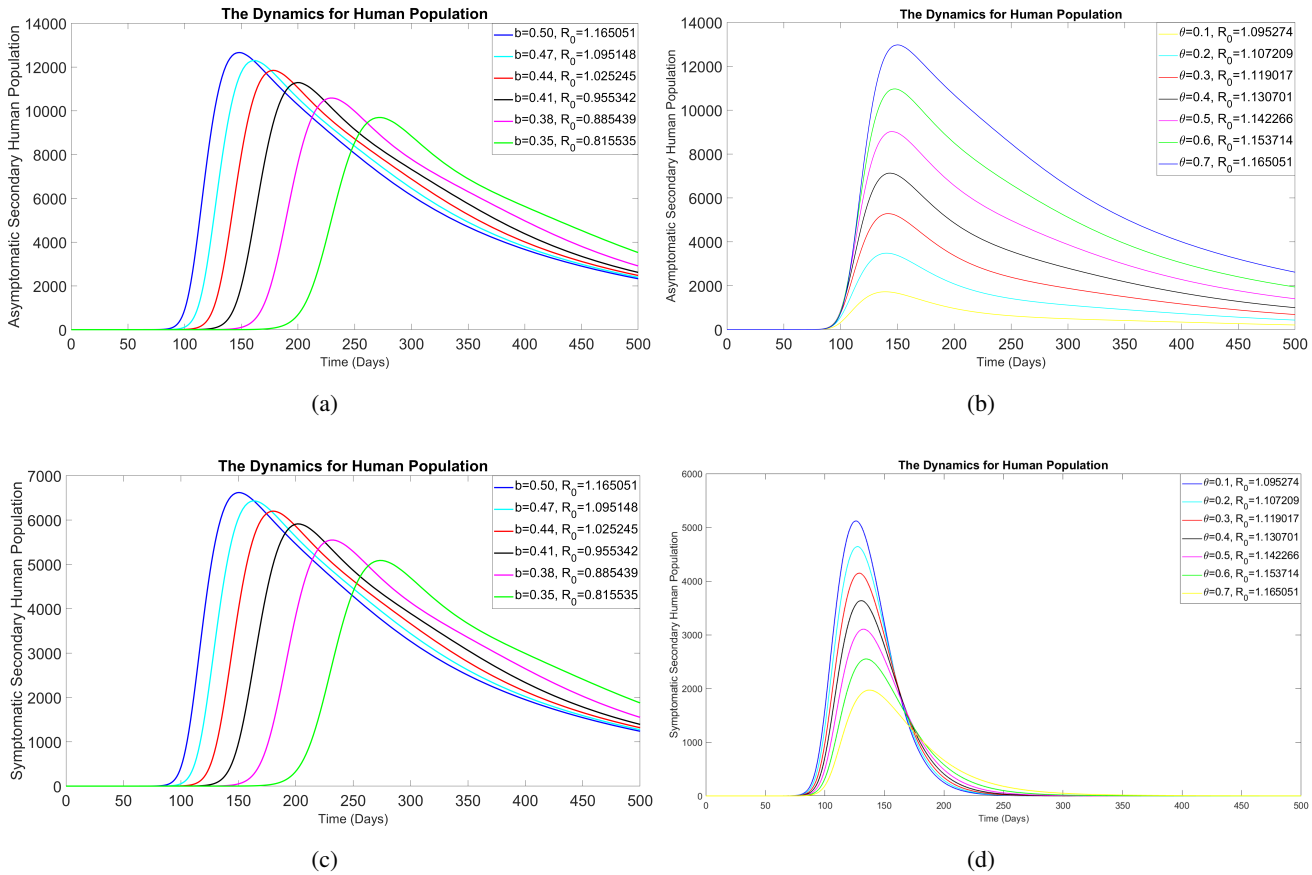

Figure 10. Effects of the biting rate b, and θ on the human population.

Figure 10(a) demonstrates that a systematic reduction in the mosquito biting rate produces a consequent decline in both the asymptomatic and symptomatic secondary human population compartments, provided that the magnitude of the reduction is sufficient to suppress $\mathcal{R}_0$ below the critical threshold of unity. This observation corroborates the epidemiological significance of vector control interventions targeting the biting rate as a viable strategy for curtailing secondary infection dynamics.

Figure 10(d) illustrates that the prevalence of asymptomatic infections within the host population exerts a discernible influence on the overall transmission dynamics of dengue fever, wherein an incremental increase in the proportion of asymptomatic cases corresponds to a marginal but measurable elevation in the basic reproduction number $\mathcal{R}_0$. Notably, variations in the parameter θ do not precipitate substantial changes in $\mathcal{R}_0$, a finding attributable to the compensatory relationship between asymptomatic and symptomatic infections' prevalence.

The demonstrated influence of η on disease dynamics indicates that elevated transmission rates from asymptomatic individuals constitute a significant driver of an epidemic's propagation within the host population. As a consequence, interventions aimed at early identification and clinical management of asymptomatic cases are an essential dengue fever control strategy, particularly in endemic settings where asymptomatic transmission may silently perpetuate the disease's persistence and impede eradication efforts.

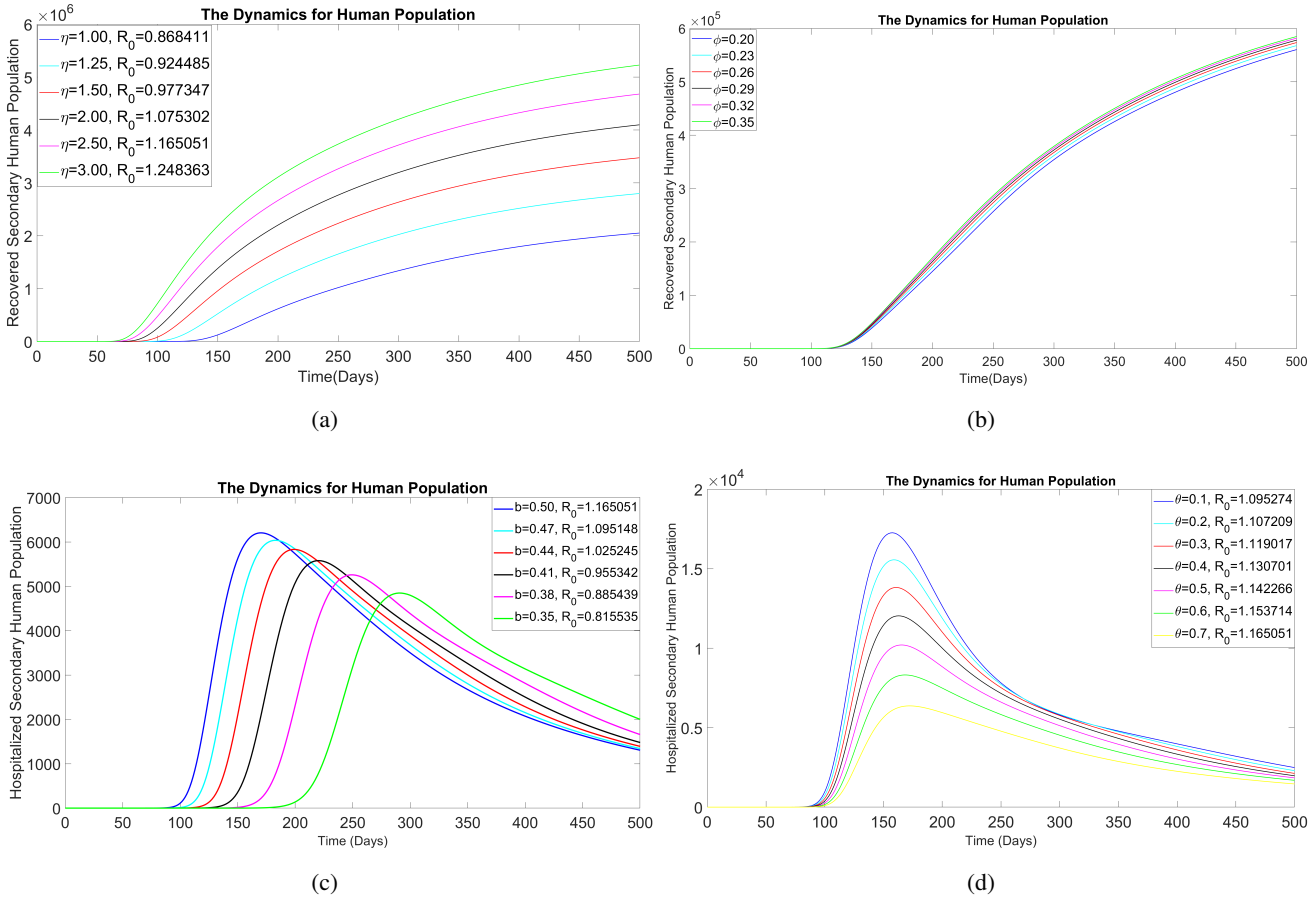

Figure 11. Effects of the biting rate b and θ on the human population.

Figure 11(a) illustrates the effect of variations in the asymptomatic modification parameter η on the recovered secondary human population compartment. Elevated values of η are associated with a progressive increase in the number of recovered individuals, a finding that underscores the epidemiological significance of silent transmission as a hidden yet consequential driver of dengue fever's dynamics.

Figure 11(b) illustrates the influence of the ADE phenomenon on the temporal dynamics of the recovered individual compartment. The results indicate that at the initial stages of the epidemic, ADE does not exert a discernible influence on the disease's dynamics. However, over an extended temporal horizon, the cumulative effect of ADE becomes increasingly apparent in shaping disease progression as secondary susceptible individuals accumulate.

Figure 11(c) demonstrates the effect of progressive reductions in the mosquito biting rate on the hospitalized secondary human population compartment, revealing that vector control interventions targeting the biting rate are effective in reducing the burden of severe dengue fever cases requiring hospitalization. Figure 11(d) illustrates that elevated values of the asymptomatic proportion parameter θ correspond to a reduction in the symptomatic secondary human population, with an associated decrease in the number of hospitalized individuals. This observation is consistent with the model assumption that asymptomatic individuals do not progress to severe dengue fever and therefore do not contribute to the hospitalized population compartment.

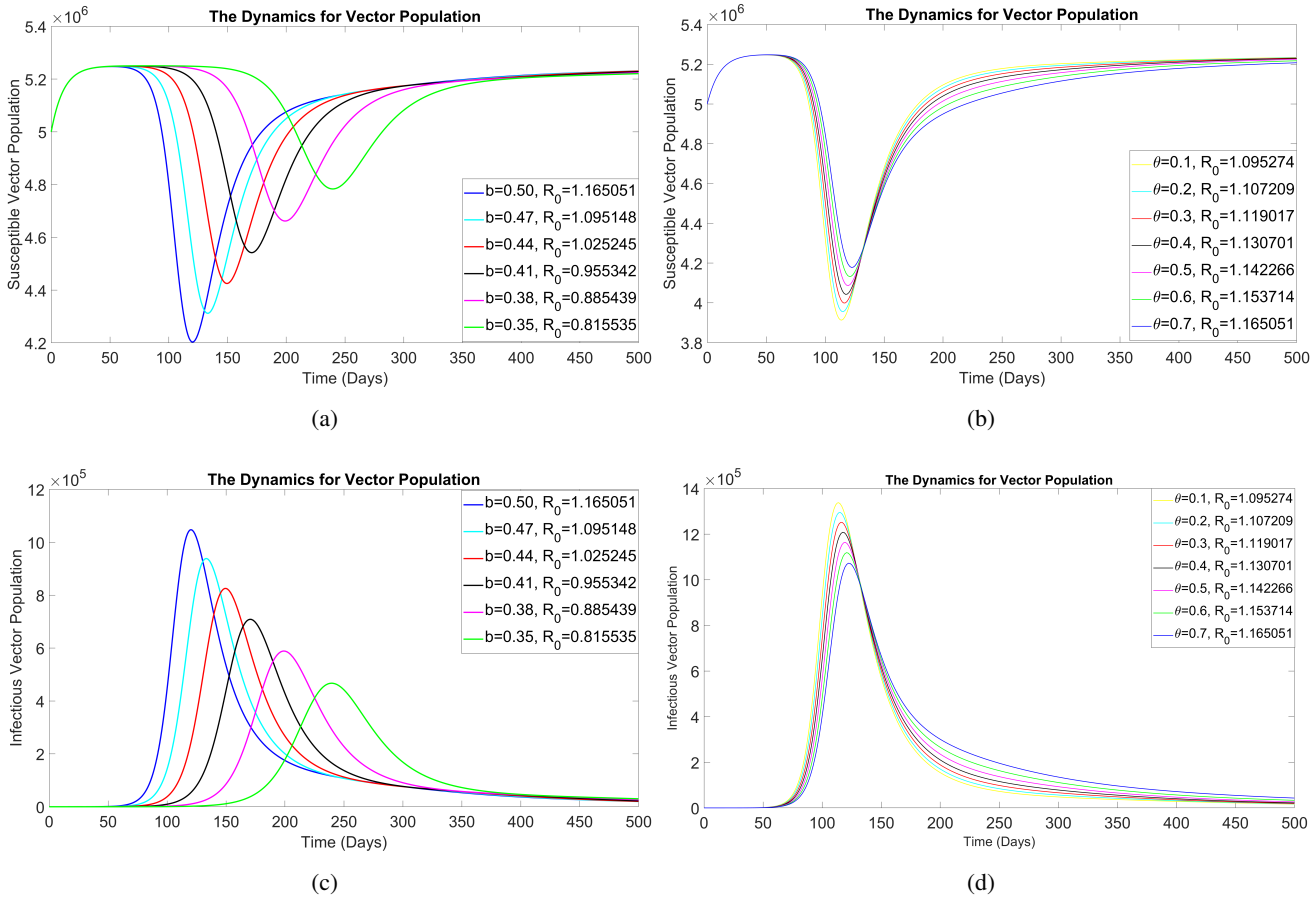

Figure 12. Effects of the biting rate b and θ on the dynamics of the vector population.

Figure 12(a), (c) illustrates the temporal dynamics of the vector population in relation to values of b, the mosquito biting rate, that yield values of $\mathcal{R}_0$ below the critical threshold of unity. Elevated magnitudes of the biting rate, corresponding to $\mathcal{R}_0 > 1$, are associated with accelerated disease transmission within the vector population, as evidenced by a precipitous decline in the susceptible vector compartment and a sharp rise in the infectious vector population. Conversely, progressive reductions in the biting rate to values sufficient to suppress $\mathcal{R}_0$ below unity are associated with decreased disease progression, a diminished proportion of infected vectors, and a correspondingly gradual depletion of the susceptible vector population.

Figure 12(b), (d) depicts the dynamics of the susceptible and infectious vector population compartments in relation to variations in the asymptomatic proportion parameter θ. The results reveal that substantial changes in θ produce only marginal changes in the dynamics of both vector population compartments. This observation, while seemingly paradoxical, is nonetheless consistent with the findings of the global sensitivity analysis of $\mathcal{R}_0$ conducted using the Latin hypercube sampling technique, which confirmed that θ exerts a statistically discernible, albeit relatively modest, influence on $\mathcal{R}_0$. The limited impact of θ on the vector's population dynamics suggests that while the proportion of asymptomatic infections modulates disease transmission at the host level, its direct effect on the vector's infection dynamics is comparatively decreased, underscoring the differential sensitivity of the host and vector compartments to changes in this epidemiological parameter.

10.3. Surface and contour plots

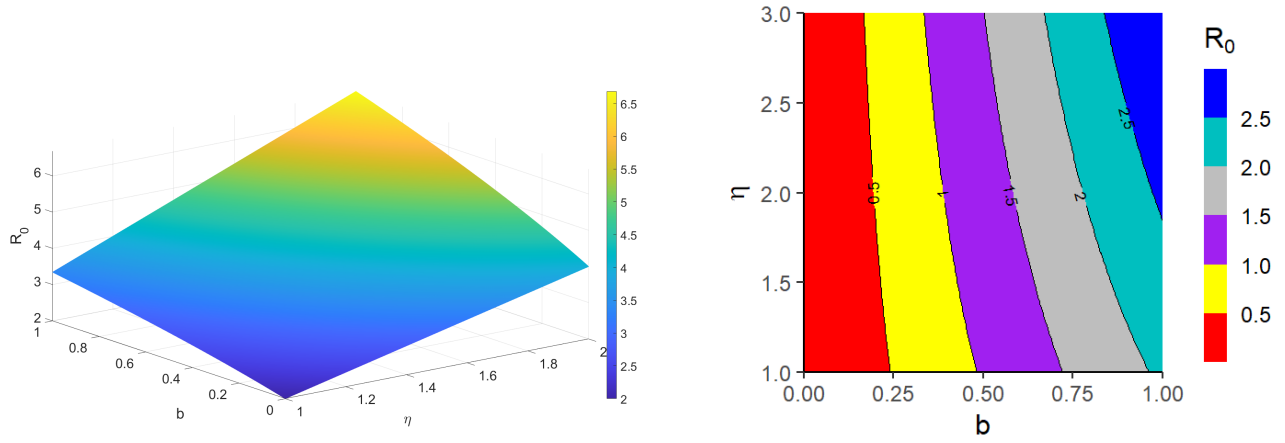

Figure 13. Three-dimensional plots and contour plots for $\mathcal{R}_0$ parameters.

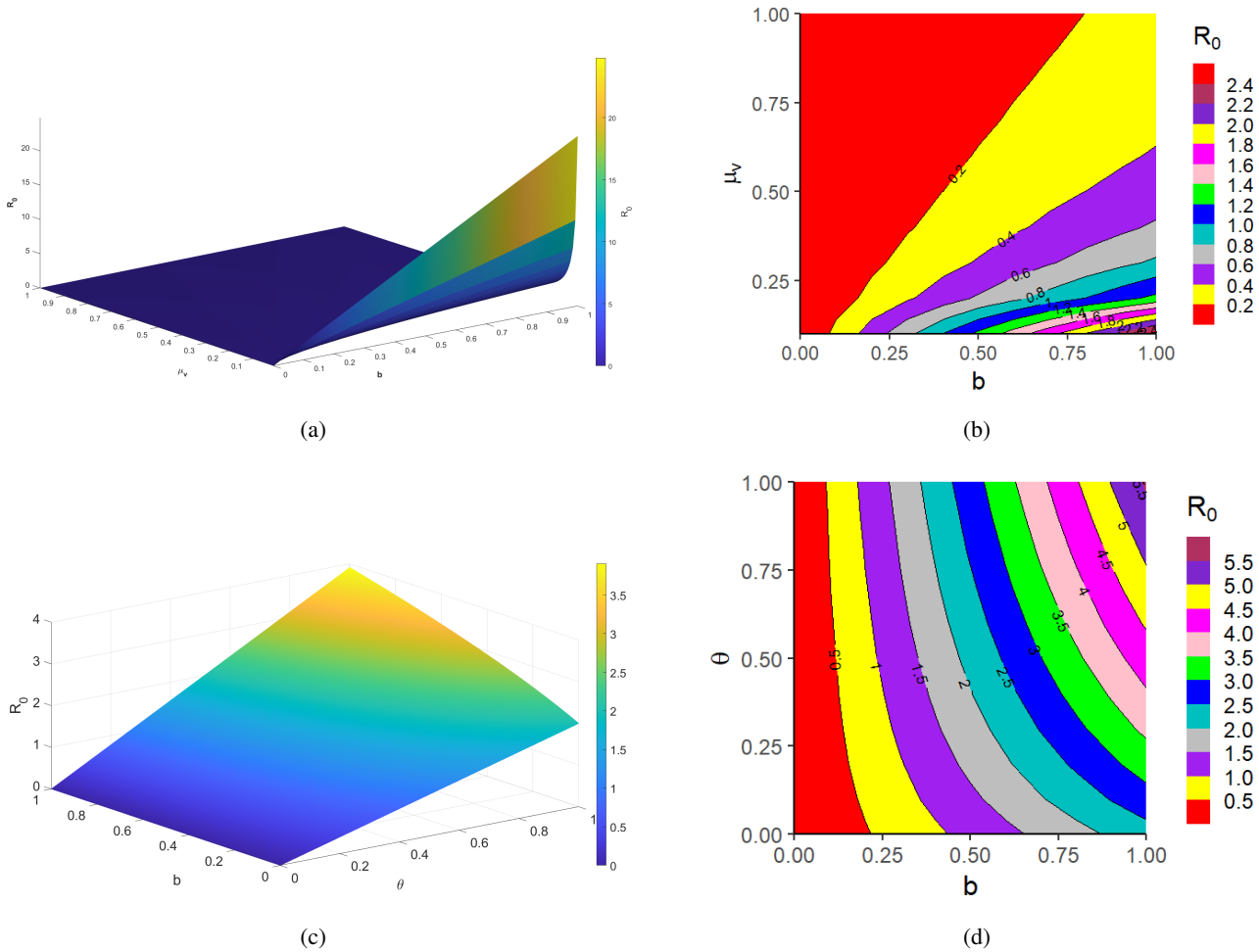

Figure 14. Three-dimensional plots and contour plots for $\mathcal{R}_0$ parameters.

10.4. Surface and contour plots

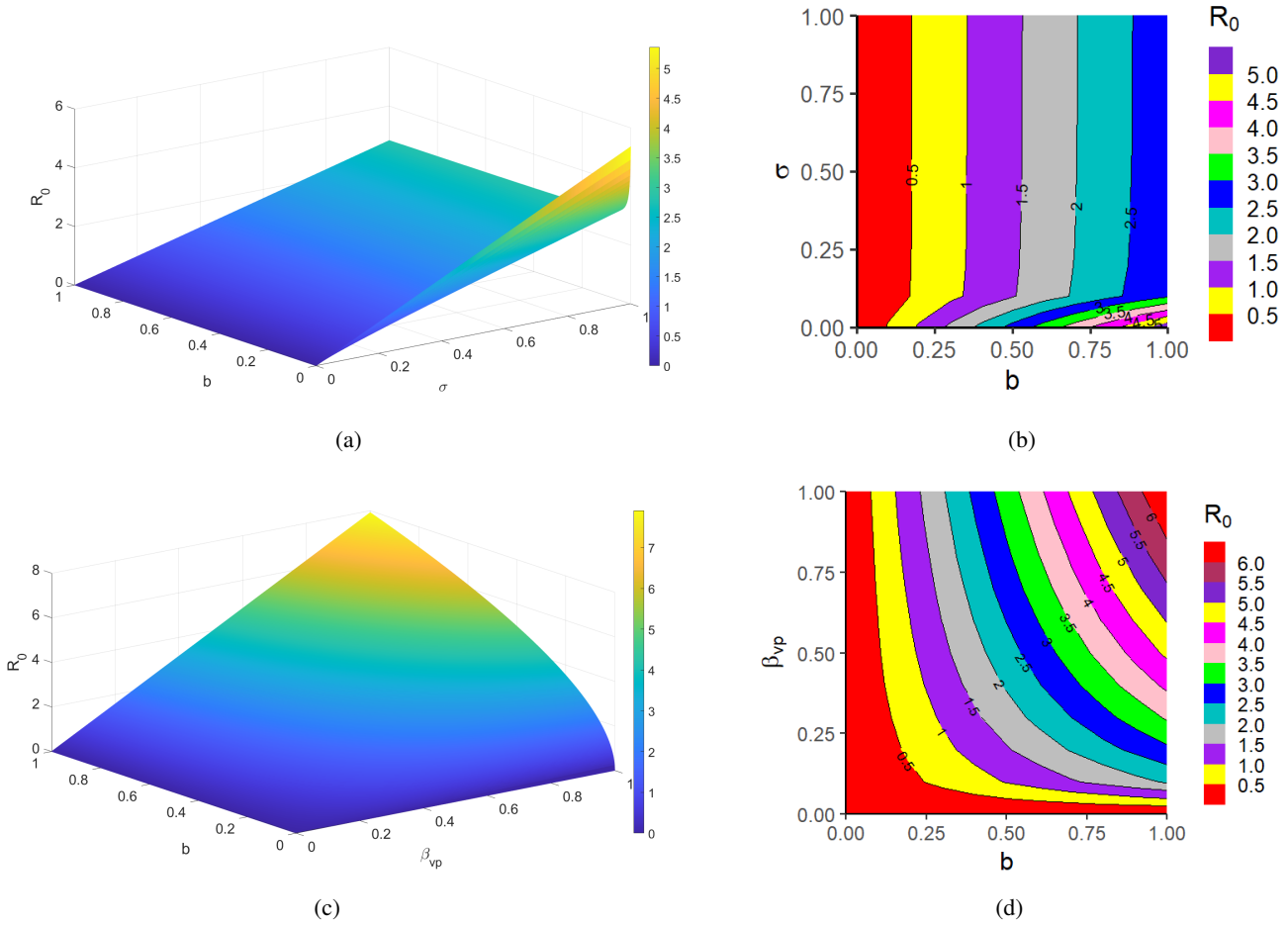

Figure 15. Three-dimensional plots and contour plots for $\mathcal{R}_0$ parameters.

The contour plots present the variation of $\mathcal{R}_0$ with respect to the key model parameters. Figure 13(a), (b) shows that a combination of a low η and a biting rate b below 0.5 is sufficient to reduce $\mathcal{R}_0$ below unity, while higher values of η necessitate more substantial reductions in b to achieve the same effect.

Figure 14(a), (b) demonstrates that elevated mosquito mortality rates μ_v effectively suppress $\mathcal{R}_0$ below unity even at relatively high biting rates. Figure 14(c), (d) shows that while reductions in θ produce a corresponding decrease in $\mathcal{R}_0$, the complementary relationship between θ and ρ limits the overall impact of this reduction on disease control. Notably, a biting rate $b < 0.25$ maintains $\mathcal{R}_0 < 1$ regardless of the value of θ.

Figure 15(c), (d) illustrates that maintaining $b < 0.25$ suppresses $\mathcal{R}_0$ below unity irrespective of β_{vp}; independently, values of $\beta_{vp} < 0.11$ are also sufficient to achieve $\mathcal{R}_0 < 1$. A linear increase in either parameter elevates $\mathcal{R}_0$ above unity, with changes in b exerting a disproportionately greater influence on overall transmission dynamics.

10.5. Scatter plots

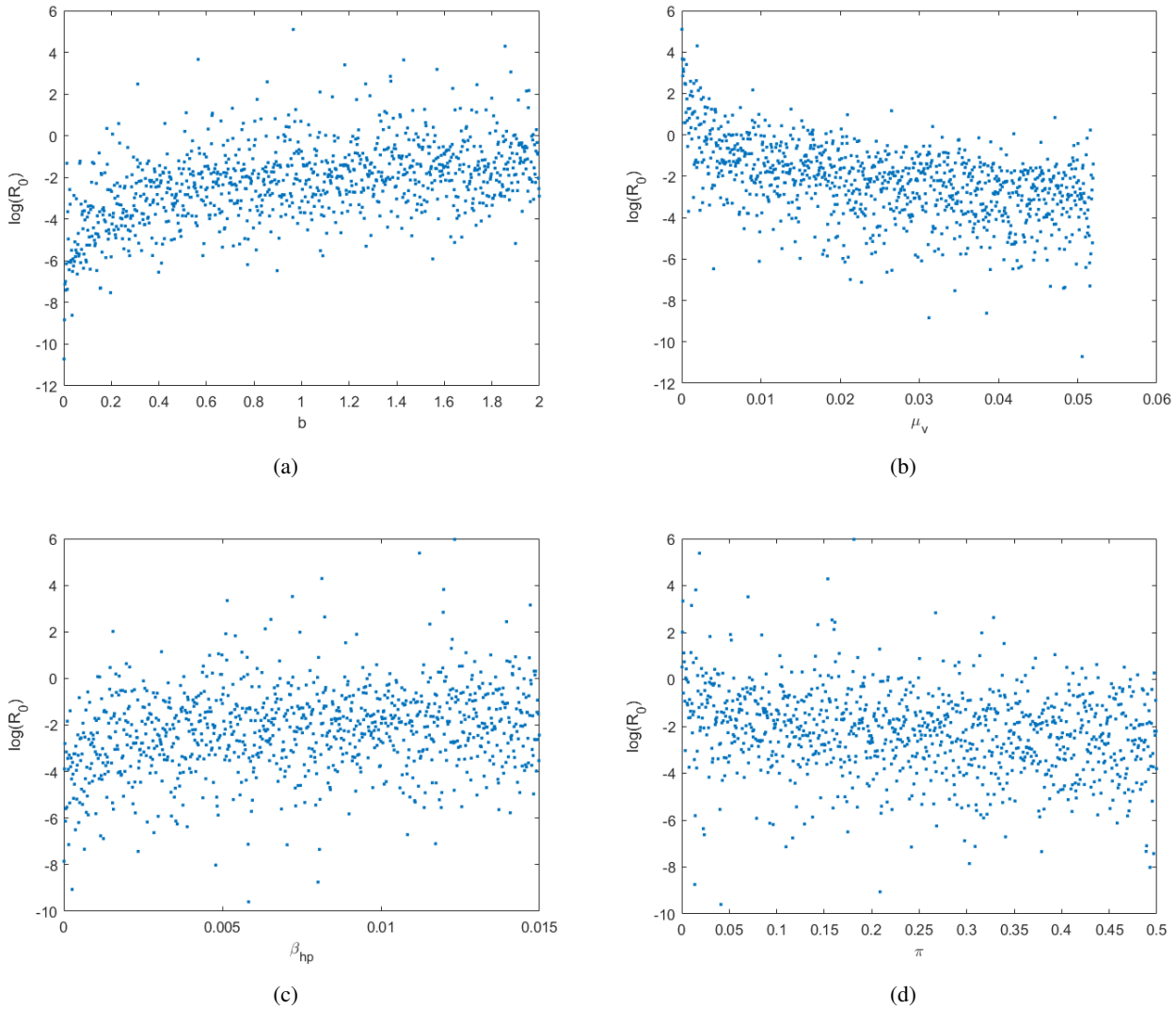

Figure 16. Scatter plots for influential basic reproduction number parameters.

10.6. Model sensitivity analysis

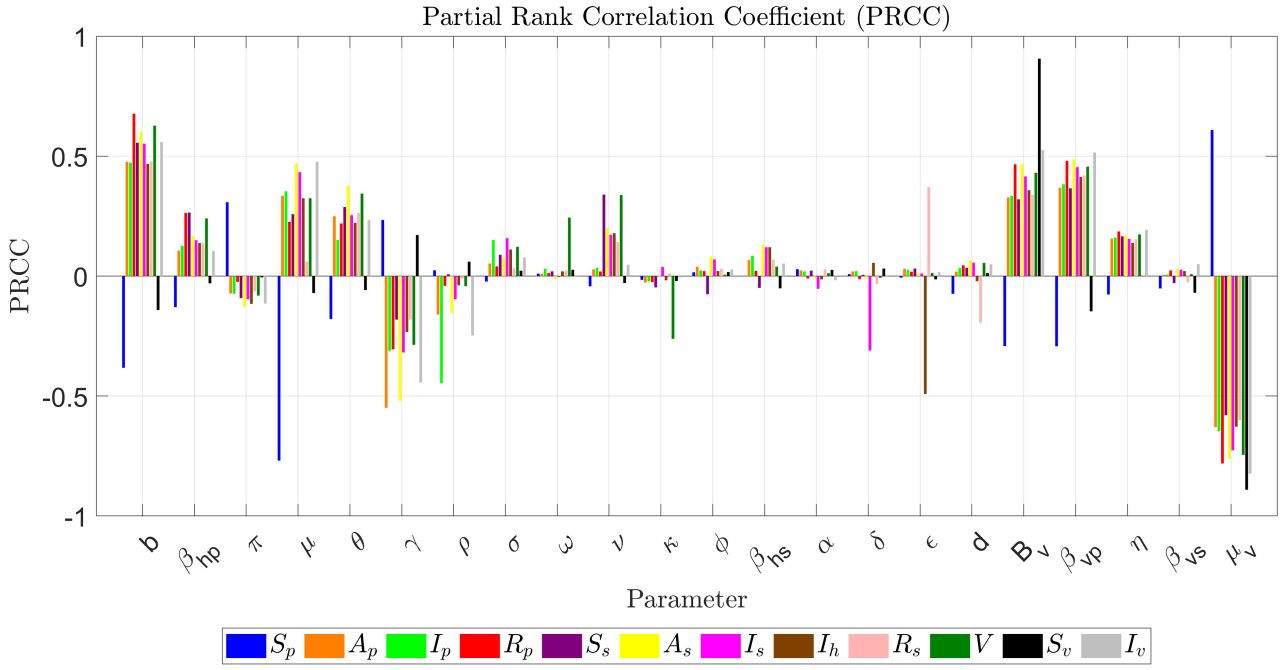

Figure 17. Model PRCC.

The sensitivity analysis presented in this section aimed to assess the robustness of the model to variations in the parameter values, thereby identifying the parameters of greatest significance to the overall model dynamics. The Latin hypercube sampling method, widely applied in both continuous and discrete epidemiological modeling frameworks, was used for this purpose. A sample size of 1000 values was generated under a uniform distribution for each model parameter, with statistical significance determined by a p-value threshold of less than 1%. Parameters were deemed epidemiologically influential if their corresponding PRCC values satisfied $|PRCC| > 0.4$, with associated p-values of $p < 0.01$. The results of the analysis are presented as a PRCC plot in Figure 17, with detailed PRCC and p-values tabulated in Table 5, Table 6, and Table 7 in the Supplementary Material, where the PRCC values are highlighted in blue and p-values in red. Parameters satisfying $|PRCC| > 0.4$ with $p < 0.01$ are identified as the primary sources of uncertainty in the corresponding model variables. The analysis identified the following parameters as the most influential determinants of model dynamics: The mosquito biting rate b, the human recruitment rate π, the recovery rate for symptomatic cases σ, the natural vector mortality rate μ_v, the proportion of asymptomatic cases θ, the recovery rate for hospitalized severe dengue cases ϵ, and the per capita transmission rate of primary infections from the host to vector β_{vp}.

11. Global sensitivity analysis

The sensitivity analysis was done through the implementation of the FME package in R [34], and the results are presented in the following figures. The 12 different graphs illustrate the uncertainty in the model that we developed. For each of the presented graphs, the variability in the model output is shown using confidence intervals. Wide confidence intervals, as observed in other compartments, show increased model variability in the model output when the parameters in Table 4 are used. The variability in the parameters was obtained through the use of data that was generated under a uniform distribution with a standard deviation of 20% around the mean value or true model output. These changes in the model output are expected, as our model is dependent on each of the parameters, thus changes in these parameters are expected to lead to changes in the model. Though these changes are expected, it is important to note that minor changes in one parameter can be counterpoised by congruous changes in the other model parameters, given a linearly dependent sensitivity function, as explained in [35].

11.1. The model's global sensitivity

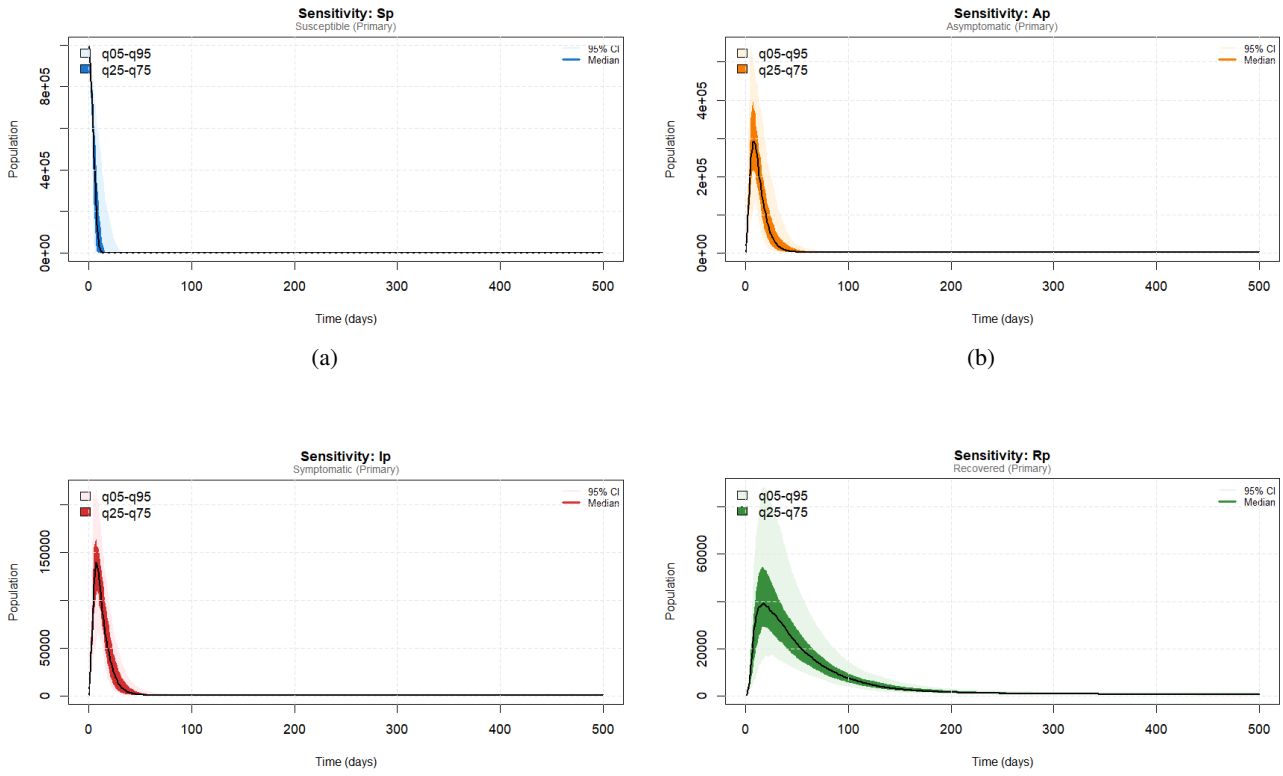

Figure 18. Global sensitivity analysis graphs.

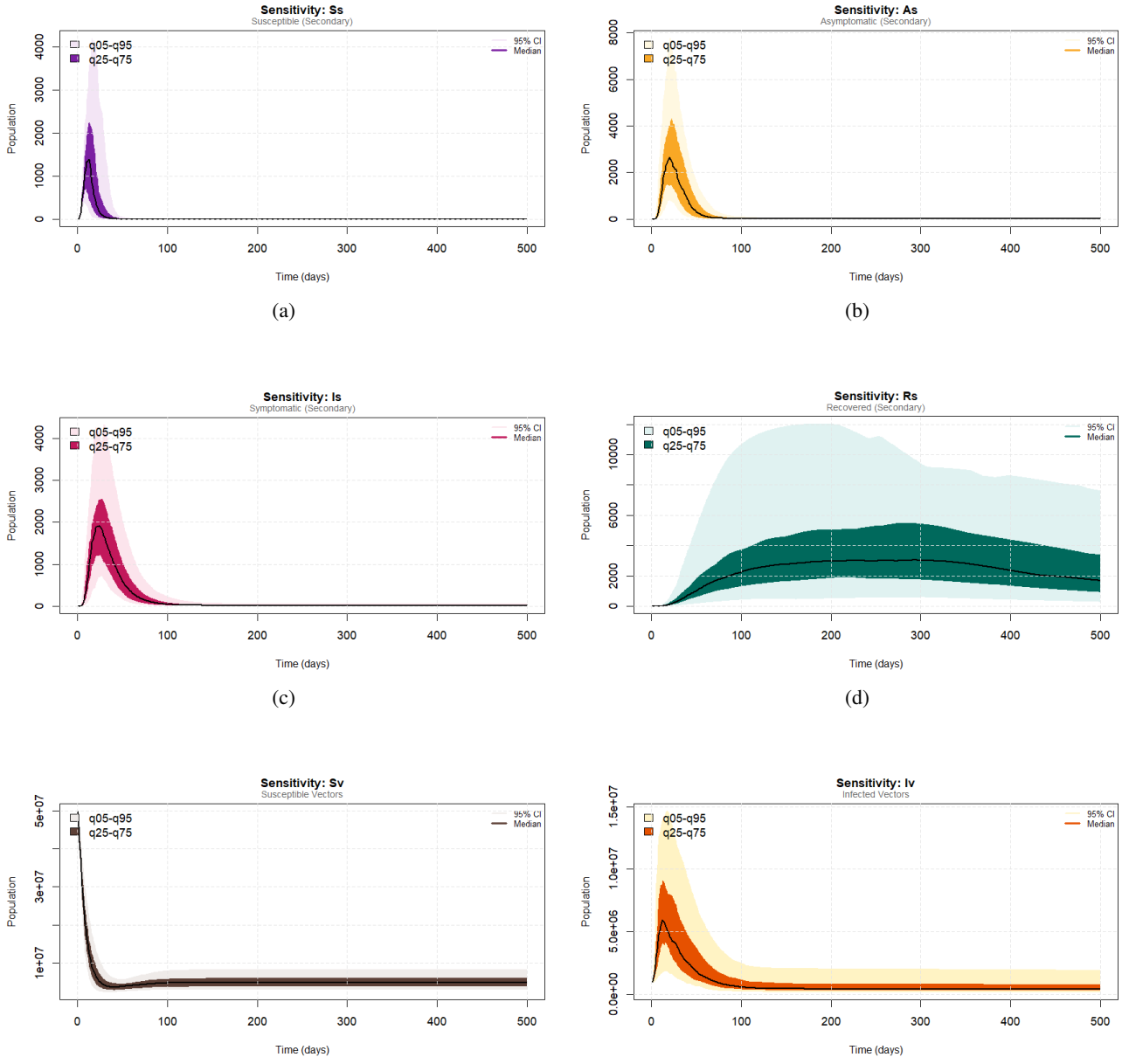

Figure 19. Global sensitivity analysis graphs.

11.2. Visualizations of the coefficient of variation

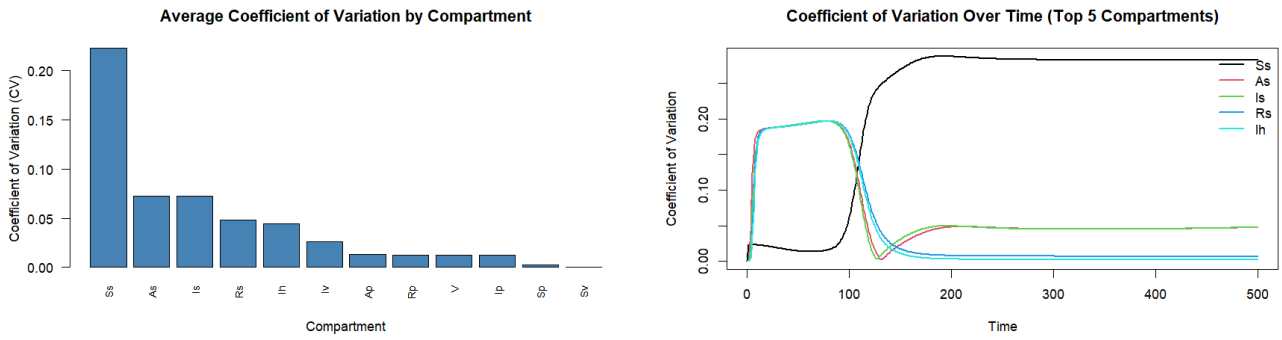

(a) (b)

Figure 20. Coefficient of variation.

In the present analysis, a temporal horizon of 500 days was adopted for the numerical simulations. The susceptible compartments S_p and S_v exhibited relatively low variability, as quantified by the average coefficient of variation (CV), a statistical measure of relative dispersion defined as the ratio of the standard deviation to the mean. In contrast, the secondary susceptible human compartment S_s, the recovered secondary compartment R_s, and the secondary active infectious compartments A_s and I_s demonstrated the highest sensitivity, indicating that these epidemiological classes constitute the primary sources of model uncertainty. The epidemiological implications of these observations are considerable. Elevated CV values associated with the aforementioned compartments indicate that the dynamics of secondary infections are subject to substantial temporal fluctuations, rendering the long-term prediction of secondary infection trajectories inherently challenging. This heightened unpredictability poses a significant challenge to public health authorities, as the erratic nature of secondary infections' dynamics precludes precise forecasting of epidemic peaks, thereby complicating the timely mobilization of healthcare resources, including hospital capacity expansion and the strategic deployment of other intervention measures. Not-withstanding the observed unpredictability of secondary infections' dynamics, the results simultaneously identify the specific epidemiological compartments that warrant prioritization in the formulation of targeted disease control strategies. Furthermore, in the context of the established backward bifurcation exhibited by the model, the elevated CV values observed in the infectious compartments carry particularly significant epidemiological consequences. Specifically, even when $\mathcal{R}_0$ approaches unity, the inherent variability within the infectious classes suggests that the epidemic's trajectory is more likely to culminate in a large-scale disease outbreak than to undergo natural elimination, despite the theoretical possibility of the disease dying out under such conditions. This observation further reinforces the inadequacy of solely targeting $\mathcal{R}_0 < 1$ as a control criterion in the presence of backward bifurcation, and underscores the necessity of more stringent and sustained intervention strategies for effective dengue fever management.

Conclusions

The primary objective of this study was to systematically investigate the influence of ADE and asymptomatic infections on the transmission dynamics of dengue fever within a novel sequential super-

infection mathematical modelling framework. The proposed model explicitly incorporated the mechanistic effects of ADE and asymptomatic infection on dengue fever's transmission dynamics. In the model analysis, the local asymptotic stability of the disease-free equilibrium was rigorously established through the application of the Hartman-Grobman theorem. Subsequently, a global sensitivity analysis was conducted by using the Latin hypercube sampling scheme, with the basic reproduction number $\mathcal{R}_0$ designated as the response variable. The analysis identified two parameters as the principal determinants of disease dynamics, as perturbations in these parameters exerted a direct and significant impact on the magnitude of $\mathcal{R}_0$. Specifically, the mosquito biting rate, b, and the mosquito mortality rate, μ_v, were identified as the most epidemiologically influential parameters governing the disease's transmission dynamics. The model analysis of primary infections' dynamics revealed that the system exhibits transcritical bifurcation at the threshold $b \approx 0.42$ at which $\mathcal{R}_0 = 1$. A particularly noteworthy observation from the numerical simulations was the pronounced influence of the modification parameter η on the disease dynamics. The model demonstrated that an enhanced transmission potential of asymptomatic individuals, estimated at two- to threefold relative to symptomatic individuals, is sufficient to drive the system toward disease endemicity, underscoring the critical epidemiological role of asymptomatic transmission in sustaining dengue fever's persistence. Analysis of the full sequential-super-infection model yielded complex and epidemiologically significant dynamics. Under the assumption that disease-induced mortality is negligible relative to the total infected population size, analytical investigations demonstrated that the full system undergoes backward bifurcation under specific parameter conditions. To verify the existence and characterize the extent of this bifurcation phenomenon, a robustness analysis was conducted, which confirmed that the backward bifurcation was strong, with the strength of robustness varying for different values of the biting rate b, for specific ϕ values within the range $\phi \in [0.1, 1.0]$, as evidenced by a progressively expanding basin of attraction. The presented study demonstrated that suppressing $\mathcal{R}_0$ below the critical threshold of unity through a systematic reduction in the mosquito biting rate b is insufficient for disease elimination. While such a reduction satisfies the necessary condition $\mathcal{R}_0 < 1$, the analysis revealed that an ADE value within the range $\phi \in [0.1, 1.0]$ is sufficient to increase backward bifurcation due to the mosquito biting rate b, with the corresponding critical bifurcation threshold b_c varying in the bistable region $b \in [b_c, 0.42)$ when $\mathcal{R}_0 < 1$. This implies that the disease-free equilibrium and an endemic equilibrium coexist in the bistable region $b \in [b_c, 0.42)$, rendering the condition $\mathcal{R}_0 < 1$ insufficient to guarantee the asymptotic stability of the disease-free equilibrium and, consequently, disease eradication. The epidemiological consequence of this finding is profound: In the presence of backward bifurcation induced by the biting rate b, the elimination of dengue fever demands that control interventions are aimed at achieving a value of b_c corresponding to $\mathcal{R}_c$, as this is the eradication threshold. The findings of this study suggest that beyond the well-established role of disease-induced mortality in precipitating backward bifurcation in host-vector models, sequential-super-infection within a multi-strain dengue fever modeling framework constitutes an independent mechanism capable of generating backward bifurcation given sufficient secondary infections, with potentially significant implications for the disease's persistence in a seronegative population. Our study also highlights the urgent need for public health authorities and policymakers to implement strategies aimed at reducing η to values approaching unity, so as to curtail the silent epidemic attributable to asymptomatic dengue transmission. This objective may be pursued through sustained media campaigns promoting mass public awareness and encouraging the widespread adoption of personal protective measures, including the use of insecticide-treated bed nets. Prospective

extensions of this work include the development of seasonality-incorporated models, stochastic modeling frameworks, and optimal control formulations to facilitate more efficient resource allocation in the control and management of dengue fever.

Use of AI Tools

The authors declare there was no use of artificial intelligence (AI) tools in the creation of this article.

Acknowledgments

Taurai Mademutsa would like to acknowledge the African Union through the Pan African University Institute for Basic Sciences, Technology and Innovation (PAUSTI) for the funding opportunity that has made this research possible.

Conflict of interest

The authors declare no conflict of interest.

References

1. Q. Jing, M. Wang, Dengue epidemiology, *Global Health J.*, **3** (2019), 37–45 https://doi.org/10.1016/j.glohj.2019.06.002
2. K. L. Ebi, J. Nealon, Dengue in a changing climate, *Environ. Res.*, **151** (2016), 115–123. https://doi.org/10.1016/j.envres.2016.07.026
3. S. Bhatt, P. W. Gething, O. J. Brady, J. P. Messina, A. W. Farlow, C. L. Moyes, et al., The global distribution and burden of dengue, *Nature*, **496** (2013), 504–507. https://doi.org/10.1038/nature12060
4. S. B. Halstead, Dengue Virus–Mosquito Interactions, *Ann. Rev. Entomol.*, **53** (2008), 273–291. https://doi.org/10.1146/annurev.ento.53.103106.093326
5. K. Hu, C. Thoens, S. Bianco, S. Edlund, M. Davis, J. Douglas, et al., The effect of antibody-dependent enhancement, cross immunity, and vector population on the dynamics of dengue fever, *J. Theor. Biol.*, **319** (2013), 62–74. https://doi.org/10.1016/j.jtbi.2012.11.021
6. N. G. Reich, S. Shrestha, A. A. King, P. Rohani, J. Lessler, S. Kalayanarooj, et al., Interactions between serotypes of dengue highlight epidemiological impact of cross-immunity, *J. Royal Soc. Interface*, **10** (2013), 20130414. https://doi.org/10.1098/rsif.2013.0414
7. O. De Santis, N. Bouscaren, A. Flahault, Asymptomatic dengue infection rate: A systematic literature review, *Heliyon*, **9** (2023), e20069. https://doi.org/10.1016/j.heliyon.2023.e20069
8. N. Khetarpal, I. Khanna, Dengue Fever: Causes, Complications, and Vaccine Strategies, *J. Immunol. Res.*, **2016** (2016), 1–14. https://doi.org/10.1155/2016/6803098
9. M. Aguiar, N. Stollenwerk, Mathematical models of dengue fever epidemiology: Multi-strain dynamics, immunological aspects associated to disease severity and vaccines, *Commun. Biomath. Sci.*, **1** (2017), 1. https://doi.org/10.5614/cbms.2017.1.1.1

10. M. Aguiar, V. Steindorf, A. K. Srivastav, N. Stollenwerk, B. W. Kooi, Bifurcation analysis of a two infection SIR-SIR epidemic model with temporary immunity and disease enhancement, *Nonlinear Dynam.*, **112** (2024), 13621–13639. https://doi.org/10.1007/s11071-024-09710-9
11. K. E. Ocwieja, A. N. Fernando, S. Sherrill-Mix, S. A. Sundararaman, R. N. Tennekoon, R. Tippalagama, et al., Phylogeography and Molecular Epidemiology of an Epidemic Strain of Dengue Virus Type 1 in Sri Lanka, *The American Society of Tropical Medicine and Hygiene*, **91** (2014), 225–234. https://doi.org/10.4269/ajtmh.13-0523
12. A. L. St. John, A. P. S. Rathore, Adaptive immune responses to primary and secondary dengue virus infections, *Nat. Rev. Immunol.*, **19** (2019), 218–230. https://doi.org/10.1038/s41577-019-0123-x
13. S. R. Hadinegoro, J. L. Arredondo-García, M. R. Capeding, C. Deseda, T. Chotpitayasunondh, R. Dietze, et al., Efficacy and Long-Term Safety of a Dengue Vaccine in Regions of Endemic Disease, *New England J. Med.*, **373** (2015), 1195–1206. https://doi.org/10.1056/nejmoa1506223
14. P. R. Asish, S. Dasgupta, G. Rachel, B. S. Bagepally, C. P. Girish Kumar, Global prevalence of asymptomatic dengue infections–a systematic review and meta-analysis, *Int. J. Infect. Diseases*, **134** (2023), 292–298. https://doi.org/10.1016/j.ijid.2023.07.010
15. I. Ghosh, P. K. Tiwari, J. Chattopadhyay, Effect of active case finding on dengue control: Implications from a mathematical model, *J. Theor. Biol.*, **464** (2019), 50–62. https://doi.org/10.1016/j.jtbi.2018.12.027
16. J. K. K. Asamoah, E. Yankson, E. Okyere, G.-Q. Sun, Z. Jin, R. Jan, et al., Optimal control and cost-effectiveness analysis for dengue fever model with asymptomatic and partial immune individuals, *Results Phys.*, **31** (2021), 104919. https://doi.org/10.1016/j.rinp.2021.104919
17. M. Aguiar, V. Anam, K. B. Blyuss, C. D. S. Estadilla, B. V. Guerrero, D. Knopoff, et al., Mathematical models for dengue fever epidemiology: A 10-year systematic review, *Phys. Life Rev.*, **40** (2022), 65–92. https://doi.org/10.1016/j.plrev.2022.02.001
18. P. van den Driessche, J. Watmough, Further Notes on the Basic Reproduction Number, In: *Further Notes on the Basic Reproduction Number*, Springer Berlin Heidelberg, 2008, 159–178. https://doi.org/10.1007/978-3-540-78911-6_6 .
19. J. H. Jones, Notes on R0.
20. M. Martcheva, *An Introduction to Mathematical Epidemiology*, Springer US, 2015.
21. B. Anderson, J. Jackson, M. Sitharam, Descartes' Rule of Signs Revisited, *Am. Math. Monthly*, **105** (1998), 447–451. https://doi.org/10.1080/00029890.1998.12004907
22. H. Kitano, Biological robustness, *Nat. Rev. Genet.*, **5** (2004), 826–837. https://doi.org/10.1038/nrg1471
23. H. Kitano, Towards a theory of biological robustness, *Molecular Syst. Biol.*, **3** (2007). https://doi.org/10.1038/msb4100179
24. M. Aguiar, S. Ballesteros, B. W. Kooi, N. Stollenwerk, The role of seasonality and import in a minimalistic multi-strain dengue model capturing differences between primary and secondary infections: Complex dynamics and its implications for data analysis, *J. Theor. Biol.*, **289** (2011), 181–196. https://doi.org/10.1016/j.jtbi.2011.08.043
25. B. Adams, M. Boots, Modelling the relationship between antibody-dependent enhancement and immunological distance with application to dengue, *J. Theor. Biol.*, **242** (2006), 337–346. https://doi.org/10.1016/j.jtbi.2006.03.002

26. M. Andraud, N. Hens, C. Marais, P. Beutels, Dynamic Epidemiological Models for Dengue Transmission: A Systematic Review of Structural Approaches, *PLoS ONE*, **7** (2012), e49085. https://doi.org/10.1371/journal.pone.0049085
27. B. Tang, Y. Xiao, S. Tang, J. Wu, Modelling weekly vector control against Dengue in the Guangdong Province of China, *J. Theor. Biol.*, **410** (2016), 65–76. https://doi.org/10.1016/j.jtbi.2016.09.012
28. M. L. Ndeffo Mbah, D. P. Durham, J. Medlock, A. P. Galvani, Country- and age-specific optimal allocation of dengue vaccines, *J. Theor. Biol.*, **342** (2014), 15–22. https://doi.org/10.1016/j.jtbi.2013.10.006
29. M. H. Zahid, H. Van Wyk, A. C. Morrison, J. Coloma, G. O. Lee, V. Cevallos, et al., The biting rate of Aedes aegypti and its variability: A systematic review (1970–2022), *PLOS Neglected Trop. Diseases*, **17** (2023), e0010831. https://doi.org/10.1371/journal.pntd.0010831
30. D. S. Shepard, E. A. Undurraga, Y. A. Halasa, J. D. Stanaway, The global economic burden of dengue: A systematic analysis, *Lancet Infect. Diseases*, **16** (2016), 935–941. https://doi.org/10.1016/s1473-3099(16)00146-8
31. S. Velumani, Y. X. Toh, S. Balasingam, S. Archuleta, Y. S. Leo, V. C. Gan, et al., Low antibody titers 5 years after vaccination with the CYD-TDV dengue vaccine in both pre-immune and naïve vaccinees, *Human Vaccines & amp; Immunotherapeutics*, **12** (2016), 1265–1273. https://doi.org/10.1080/21645515.2015.1126012
32. S. Lee, C. Castillo-Chavez, The role of residence times in two-patch dengue transmission dynamics and optimal strategies, *J. Theor. Biol.*, **374** (2015), 152–164. https://doi.org/10.1016/j.jtbi.2015.03.005
33. P. Pongsumpun, I.-M. Tang,N. Wongvanich, Optimal control of the dengue dynamical transmission with vertical transmission, *Adv. Differ. Equat.*, **2019** (2019). https://doi.org/10.1186/s13662-019-2120-6
34. K. Soetaert, T. Petzoldt, Inverse Modelling, Sensitivity and Monte Carlo Analysis inRUsing PackageFME, *J. Stat. Software*, **33** (2010). https://doi.org/10.18637/jss.v033.i03
35. M. Omlin, R. Brun, P. Reichert, Biogeochemical model of Lake Zürich: Sensitivity, identifiability and uncertainty analysis, *Ecol. Model.*, **141** (2001), 105–123. https://doi.org/10.1016/s0304-3800(01)00257-5

AIMS Press